

Electrical resistance under pressure in textured $\text{Bi}_2\text{Sr}_2\text{CaCu}_2\text{O}_{8+y}$: Enhancement of the energy gap and thermodynamic fluctuations

Q. Wang, G. A. Saunders, H. J. Liu, M. S. Acres, and D. P. Almond

Schools of Physics and Materials Science, University of Bath, Claverton Down, Bath BA2 7AY, United Kingdom

(Received 3 September 1996)

The effects of hydrostatic pressure up to 1 GPa on the ab -plane electrical resistance of textured $\text{Bi}_2\text{Sr}_2\text{CaCu}_2\text{O}_{8+y}$ have been measured. Use of the Ambegaokar-Halperin (AH) model to examine the pressure effects on weak links across grain boundary leads to a value of $0.12 \pm 0.02 \text{ GPa}^{-1}$ for the pressure derivative $d[\ln\Delta_j(0)]/dP$ of the energy gap $\Delta_j(0)$ at junctions formed by grains; $\Delta_j(0)$ for $\text{Bi}_2\text{Sr}_2\text{CaCu}_2\text{O}_{8+y}$ is about 10 times smaller than that of $\text{YBa}_2\text{Cu}_3\text{O}_{7-\delta}$. The thermodynamic fluctuations of the superconducting order parameter have a two-dimensional character above T_c and below 115 K. Applying hydrostatic pressure enhances the thermodynamic fluctuations: creation of the superconducting quasiparticles well above T_c is enhanced under pressure. As pressure is increased, the characteristic thickness d of the two-dimensional system decreases nonlinearly by about 20% up to 0.71 GPa. The pressure derivatives dT_c/dP of the superconducting transition temperature T_c have been determined as $1.6 \pm 0.3 \text{ KGPa}^{-1}$, $1.8 \pm 0.2 \text{ KGPa}^{-1}$, and $3.0 \pm 0.2 \text{ KGPa}^{-1}$ at the onset, midpoint, and offset of the R - T curve, respectively. Thermodynamic fluctuations affect dT_c/dP at onset. The large value of dT_c/dP at offset is due to the influence of the weak links at grain boundaries. A value of -1.4 is obtained for $d \ln T_c / d \ln V$, which, like that for monocrystalline $\text{Bi}_{2.2}(\text{Sr,Ca})_{2.8}\text{Cu}_2\text{O}_{8+y}$, falls between those predicted by the BCS and the resonating valence-bond theories. In the normal state $d \ln \rho_{ab} / dP$ is $-8.4\% \pm 0.2 \text{ GPa}^{-1}$ at 293 K and $d \ln R_{ab} / d \ln V$ is 2.01 ± 0.06 . The pressure derivative $d \ln R_{ab} / dP$ of the normal-state resistance of textured $\text{Bi}_2\text{Sr}_2\text{CaCu}_2\text{O}_{8+y}$ shows a temperature dependence, which is affected by applied pressure and thermodynamic fluctuations. [S0163-1829(97)01513-0]

I. INTRODUCTION

We have recently reported¹ a detailed hydrostatic pressure investigation of the superconducting phase-transition temperature T_c and the normal-state resistance of monocrystalline $\text{Bi}_{2.2}(\text{Sr,Ca})_{2.8}\text{Cu}_2\text{O}_{8+y}$. However, polycrystalline textured high- T_c materials are more likely to find industrial applications and these materials have important microstructural differences that alter their electrical properties significantly from those obtained from measurements of single-crystal samples. These ceramics, which consist of superconducting grains and contain pores and microcracks, exhibit complex behavior associated with these defects, quite different in kind from that of single crystals. This behavior is attributed to thermodynamic fluctuations of the superconducting order parameter which affect the electrical resistance characteristics in both normal and superconducting states. Application of pressure influences these structural defects, especially interactive features across grain boundaries. Hence, it is instructive to compare the effects of pressure on the electrical properties of textured ceramics with those obtained for single crystals. A central objective is to investigate effects of pressure on the weak-link properties, which determine the transport critical-current density J_c at low magnetic field in polycrystalline materials,² a major factor in limiting the application of high- T_c superconducting materials.

II. EXPERIMENT

The samples of textured $\text{Bi}_2\text{Sr}_2\text{CaCu}_2\text{O}_{8+y}$ were prepared at Argonne National Laboratory by the sinter-forging method.³ An x-ray-diffractometry study showed that their

structural characteristics are similar to those obtained on another very dense textured $\text{Bi}_2\text{Sr}_2\text{CaCu}_2\text{O}_{8+y}$ sample (Fig. 1 in Ref. 4). A large proportion of the grains are aligned preferentially with the ab plane parallel to the top faces of the sample, while the c axis is perpendicular to these faces, along the sinter-forging direction. The electrical resistance of the textured sample was measured using a conventional four-point configuration aligned along the largest sample dimension. The major contribution to the measured electrical resistance R is R_{ab} in the ab plane, corresponding to a resistivity ρ_{ab} . The methods and procedures used to make electrical contacts and to measure the effects of hydrostatic pressure on the electrical resistance have been described elsewhere.¹

III. RESULTS

Typical measurements of the temperature dependence of the electrical resistance R_{ab} at constant pressure are shown in Fig. 1. Excellent agreement was found between the data measured while decreasing or increasing temperature. For clarity, only those data measured while decreasing temperature are included in the figure.

A. Normal state

The room-temperature (293 K) pressure dependence of the normal-state resistance, R_{ab} , of the textured sample is shown in Fig. 2, with the corresponding data for the monocrystalline $\text{Bi}_{2.2}(\text{Sr,Ca})_{2.8}\text{Cu}_2\text{O}_{8+y}$.¹ Several pressure cycles were measured and marked differences were obtained while increasing and decreasing the pressure, a feature not found for monocrystalline $\text{Bi}_{2.2}(\text{Sr,Ca})_{2.8}\text{Cu}_2\text{O}_{8+y}$, whose room-

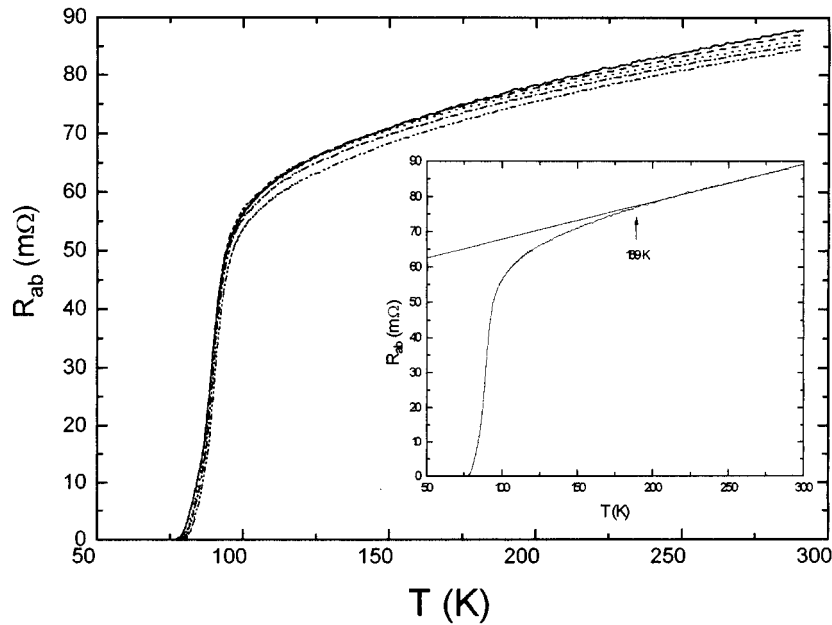


FIG. 1. The temperature dependence of the in-plane electrical resistance of textured $\text{Bi}_2\text{Sr}_2\text{CaCu}_2\text{O}_{8+y}$ under selected pressures. Solid line: $P=10^{-4}$ GPa, dashed line: $P=0.14$ GPa, dotted line: $P=0.35$ GPa, dash-dotted line: $P=0.53$ GPa, dash-double-dotted line: $P=0.71$ GPa. Inset: the deviation from linear behavior caused by thermodynamic fluctuations of the superconducting order parameter at atmospheric pressure; the arrow indicates the temperature 189 K at which deviation begins.

temperature resistance was accurately reversible during pressure cycling. The average pressure dependence $d \ln R_{ab}/dP = -6.3\% \pm 0.2 \text{ GPa}^{-1}$ of the textured sample is much smaller than that ($-25.5\% \pm 0.2 \text{ GPa}^{-1}$) of the single crystal.

The pressure dependence of the in-plane resistance R_{ab} from 100 to 290 K is shown in Fig. 3. At 290 K, R_{ab} decreases almost linearly with increasing pressure. Below about 120 K, R_{ab} starts to show an opposite behavior in the low-pressure region: R_{ab} first increases as pressure is increased, and then decreases. This behavior is quite different from that observed in monocrystalline $\text{Bi}_{2.2}(\text{Sr,Ca})_{2.8}\text{Cu}_2\text{O}_{8+y}$ for which the pressure dependence of R_a is hardly affected by temperature (Figs. 7 and 8 in Ref. 1). The temperature dependence of the pressure derivative

$d(\ln R_{ab})/dP$ of R_{ab} under selected pressures is plotted in Fig. 4, together with the temperature dependence of $d(\ln R_a)/dP$ of monocrystalline $\text{Bi}_{2.2}(\text{Sr,Ca})_{2.8}\text{Cu}_2\text{O}_{8+y}$ (Ref. 1) at atmospheric pressure. Above about 200 K at pressures lower than 0.5 GPa, the pressure derivative $d(\ln R_{ab})/dP$ is almost independent of temperature. At lower temperature, under a pressure of less than 0.2 GPa, $d(\ln R_{ab})/dP$ increases in good agreement with the expression

$$\left(\frac{d(\ln R_{ab})}{dP} \right)_{P=0} = A + B e^{-T/t}. \quad (1)$$

At atmospheric pressure $A = -0.085 \text{ GPa}^{-1}$, $B = 1.819 \text{ GPa}^{-1}$, and $t = 44.15 \text{ K}$. The relationship between

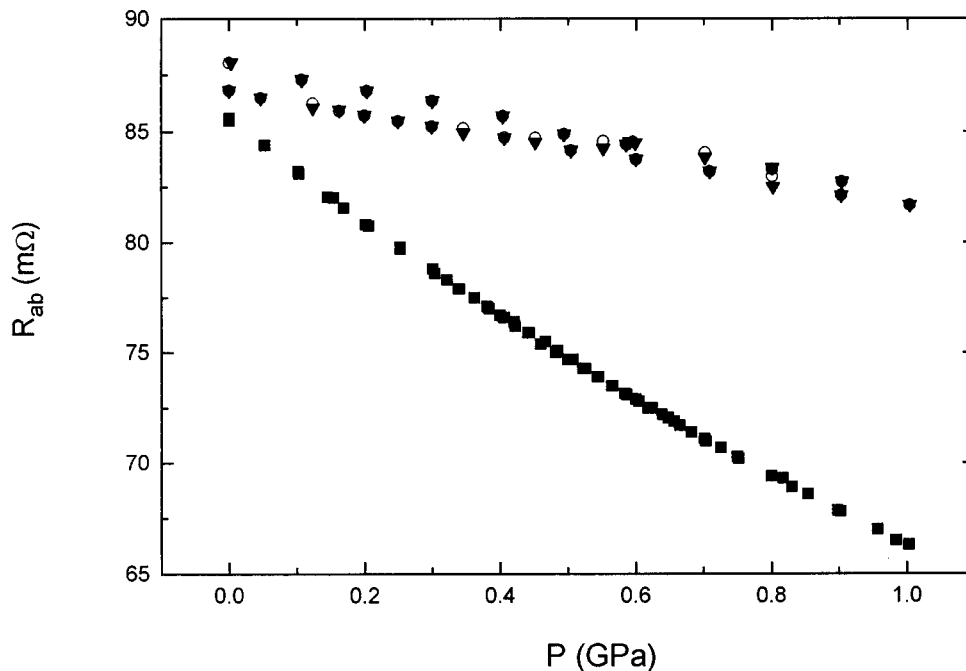


FIG. 2. The pressure dependence of the in-plane normal-state resistance at room temperature. Solid triangles: pressure cycle 1 for textured $\text{Bi}_2\text{Sr}_2\text{CaCu}_2\text{O}_{8+y}$; open circles: pressure cycle 2 for $\text{Bi}_2\text{Sr}_2\text{CaCu}_2\text{O}_{8+y}$; solid squares: pressure cycle 2 for monocrystalline $\text{Bi}_{2.2}(\text{Sr,Ca})_{2.8}\text{Cu}_2\text{O}_{8+y}$.

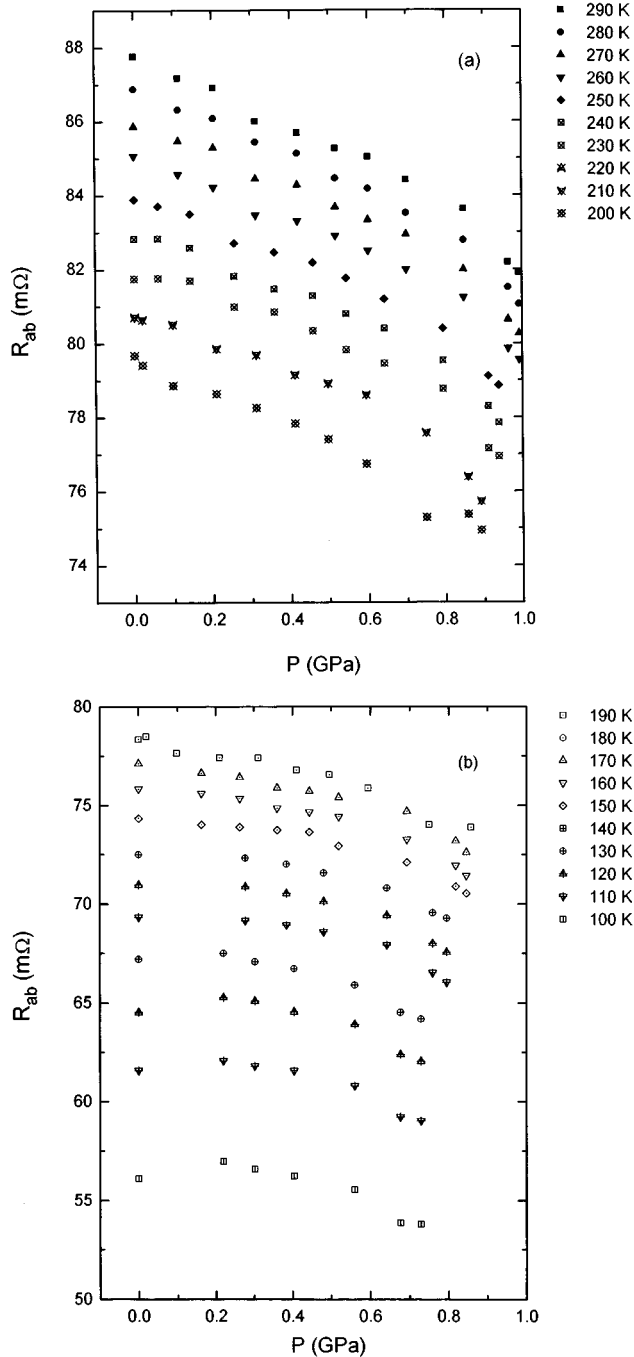


FIG. 3. The pressure dependence of the ab -plane normal-state resistance at fixed temperatures (a) from 290 to 200 K and (b) from 190 to 100 K.

$d(\ln R_{ab})/dP$ and temperature T changes to a linear form below 0.2 GPa (upright triangle Δ in Fig. 4):

$$\left(\frac{d(\ln R_{ab})}{dP}\right)_{P=0} = 1.88 \times 10^{-2} - 2.6 \times 10^{-4} T, \quad (2)$$

a very weak temperature dependence. Above 0.2 GPa, $d(\ln R_{ab})/dP$ varies nonlinearly with temperature. This non-linearity is enhanced as pressure increases (Fig. 4).

The temperature dependence of R_{ab} of textured $\text{Bi}_2\text{Sr}_2\text{CaCu}_2\text{O}_{8+y}$ was found to vary with pressure (Fig. 5),

in contrast to monocrystalline $\text{Bi}_{2.2}(\text{Sr,Ca})_{2.8}\text{Cu}_2\text{O}_{8+y}$ (Fig. 3 in Ref. 1). The temperature derivative dR_{ab}/dT for the normal-state in-plane resistance of textured $\text{Bi}_2\text{Sr}_2\text{CaCu}_2\text{O}_{8+y}$, determined using a linear regression, is plotted in Fig. 6, to show clearly the pressure effects. The temperature derivative dR_{ab}/dT shows parabolic behavior up to 0.7 GPa.

B. Superconducting state

The pressure dependences of the superconducting transition temperature, employing three commonly used conventions, are shown in Fig. 7. The three definitions of T_c are^{5,6} the onset, midpoint, and offset, being the temperatures at 90, 50, and 10 % of the normal-state resistance R_N linearly extrapolated to the transition region. The transition width ΔT_c then becomes $T_c(\text{offset}) - T_c(\text{onset})$. A linear temperature dependence is a common feature of the normal-state electrical resistance of optimally doped high-temperature superconductors and it is found at higher temperatures, from 290 to 193 K, in the textured $\text{Bi}_2\text{Sr}_2\text{CaCu}_2\text{O}_{8+y}$. The linear extrapolation of this high-temperature R_{ab} leads to transition temperatures at atmospheric pressure of $T_c(\text{onset}) = 108.2 \pm 0.2$ K, $T_c(\text{mid}) = 89.9 \pm 0.2$ K, $T_c(\text{offset}) = 82.9 \pm 0.2$ K, and $\Delta T_c = 25.3 \pm 0.2$ K.

The shapes of the R - T curve vary with pressure (Figs. 2, 5, and 6), reducing accuracy in determination of the pressure effects on $T_c(\text{onset})$ and $T_c(\text{offset})$. Each T_c value from different definitions increases linearly with pressure. $T_c(\text{onset})$ has the largest rate of increase, while $T_c(\text{mid})$ has the smallest. Linear regression of the pressure dependence of T_c gives $dT_c^{\text{on}}/dP = 5.4 \pm 0.7$ K GPa⁻¹ for $T_c(\text{onset})$, $dT_c^{\text{mid}}/dP = 2.0 \pm 0.2$ K GPa⁻¹ for $T_c(\text{mid})$ and $dT_c^{\text{off}}/dP = 3.1 \pm 0.2$ K GPa⁻¹ for $T_c(\text{offset})$. The value of dT_c^{mid}/dP is similar to most results reported for single-crystalline and polycrystalline $\text{Bi}_2\text{Sr}_2\text{CaCu}_2\text{O}_{8+y}$ (Table II in Ref. 1), but those of dT_c^{on}/dP and dT_c^{off}/dP are larger. The pressure derivative of the transition width ΔT_c is $d(\Delta T_c)/dP = 2.2 \pm 0.5$ K GPa⁻¹.

An alternative approach is to extrapolate the normal-state resistance R_N immediately above the region where the resistance drops sharply. At atmospheric pressure the T_c values and their pressure derivatives determined in this way are $T_c(\text{onset}) = 96.1 \pm 0.2$ K, $T_c(\text{mid}) = 89.2 \pm 0.2$ K, $T_c(\text{offset}) = 82.5 \pm 0.2$ K, and $\Delta T_c = 13.7 \pm 0.2$ K. The pressure derivative of ΔT_c is $d(\Delta T_c)/dP = -1.1 \pm 0.4$ K GPa⁻¹. This value of ΔT_c is similar to that reported⁶ for a Bi-Pb-Sr-Ca-Cu-O sample with a T_c of 90 K. Linear regression of the data obtained in this alternative way gives $dT_c^{\text{on}}/dP = 1.6 \pm 0.3$ K GPa⁻¹ for $T_c(\text{onset})$, $dT_c^{\text{mid}}/dP = 1.8 \pm 0.2$ K GPa⁻¹ for $T_c(\text{mid})$, and $dT_c^{\text{off}}/dP = 3.0 \pm 0.2$ K GPa⁻¹ for $T_c(\text{offset})$. The value of dT_c^{on}/dP is compatible to that reported by other authors (see Table II in Ref. 1), implying that the influence of the rounding effects on the pressure derivative dT_c^{on}/dP have been reduced. The values of dT_c^{mid}/dP and dT_c^{off}/dP are only changed slightly.

Another method used to determine T_c is to choose the temperature at which a cusp, or a maximum, appears in the gradient dR/dT in the transition region.^{7,8} The transition temperature T_c^c , with the superscript ‘‘c’’ indicating the cusp point, determined using this method at atmospheric pressure is 88.7 ± 0.2 K and its pressure derivative $dT_c^c/dP = 2.4 \pm 0.5$

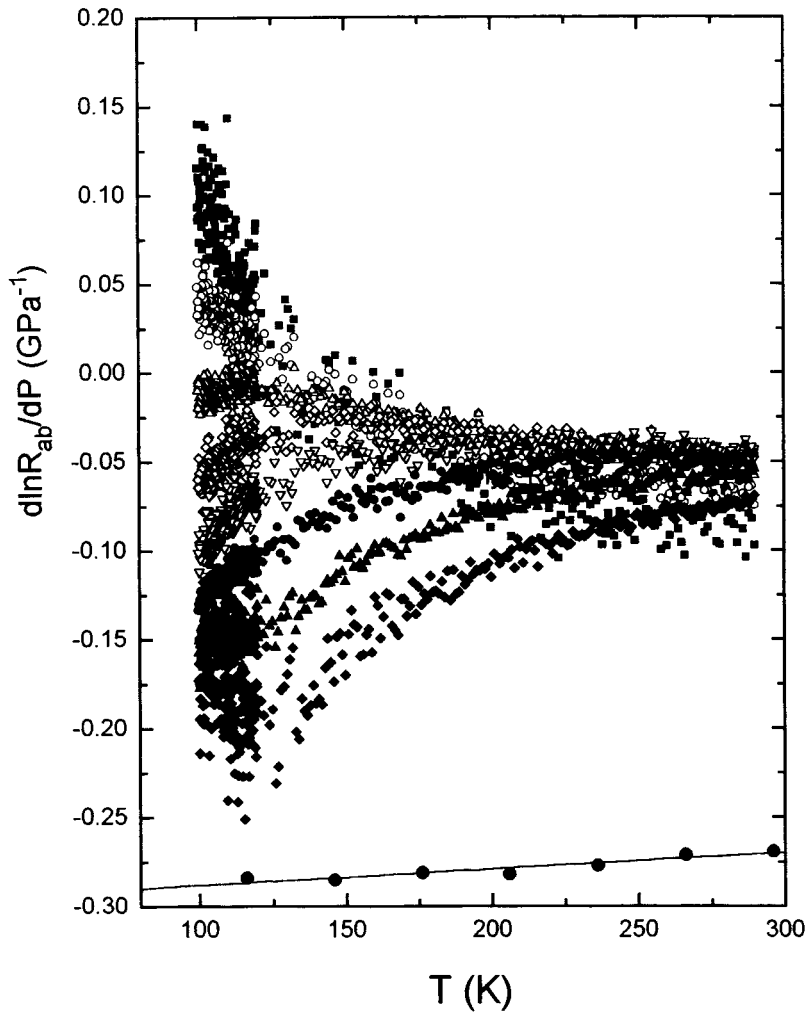


FIG. 4. The temperature dependence of the pressure derivative $d \ln R_{ab}/dP$ under different pressures. For textured $\text{Bi}_2\text{Sr}_2\text{CaCu}_2\text{O}_{8+y}$, solid square, $P=10^{-4}$ GPa; open circle, $P=0.1$ GPa; open upper-triangle, $P=0.2$ GPa; open diamond, $P=0.3$ GPa; open down-triangle, $P=0.4$ GPa; solid circle, $P=0.5$ GPa; solid upper-triangle, $P=0.6$ GPa; solid diamond, $P=0.7$ GPa. Large solid circles for monocrystalline $\text{Bi}_{2.2}(\text{Sr,Ca})_{2.8}\text{Cu}_2\text{O}_{8+y}$ at 10^{-4} GPa. The solid line shows the fit of linear regression.

KGPa^{-1} , larger than that determined by the method in the previous paragraph. Yet another approach⁹ is to take T_c as the temperature at which a straight line fit of the R - T curve of the transition range intercepts with the zero-resistance axis. This gives $T_c^0=82.6$ K and $dT_c^0/dP=3.4\pm 0.3$ KGPa^{-1} almost the same as those of $T_c(\text{offset})$ and dT_c^{off}/dP given in the last paragraph. The large value of dT_c^{off}/dP is caused by the change in the shape of the R - T curve in the lower part of the transition region. There is a tail in the R - T curve as the electrical resistance approaches zero (Fig. 1). Application of pressure increases the starting temperature of the tail and the flat part of the tail shifts to higher temperature. Thus, the temperature region ΔT_c^{off} corresponding to 10% R_N under different pressures is broadened, which leads to a large value for dT_c^{off}/dP .

Thus the different methods lead to different values of T_c . The values of T_c and its pressure derivative, determined in the upper and lower sections of the transition region, can be affected by the shape changes in the R - T curve, which are caused by nontransition effects. Specifically, the values of $T_c(\text{onset})$ and the pressure derivatives of $T_c(\text{onset})$ and $T_c(\text{offset})$ are sensitive to the variation of the resistance curve whilst the values of $T_c(\text{mid})$ (89.2 ± 0.2 K) and its pressure derivative dT_c^{mid}/dP (1.8 ± 0.2 KGPa^{-1}) are not. Although $T_c(\text{mid})$ (89.2 ± 0.2 K) determined for textured $\text{Bi}_2\text{Sr}_2\text{CaCu}_2\text{O}_{8+y}$ is similar to that (90.3 ± 0.2 K) for mono-

crystalline $\text{Bi}_{2.2}(\text{Sr,Ca})_{2.8}\text{Cu}_2\text{O}_{8+y}$,¹ the R - T curve above the transition range does not show the semiconductorlike behavior of the oxygen-deficient single crystal. In view of this and on the basis of work by Klotz and Schilling,¹⁰ textured $\text{Bi}_2\text{Sr}_2\text{CaCu}_2\text{O}_{8+y}$ used here can be considered to be slightly oxygen overdoped.

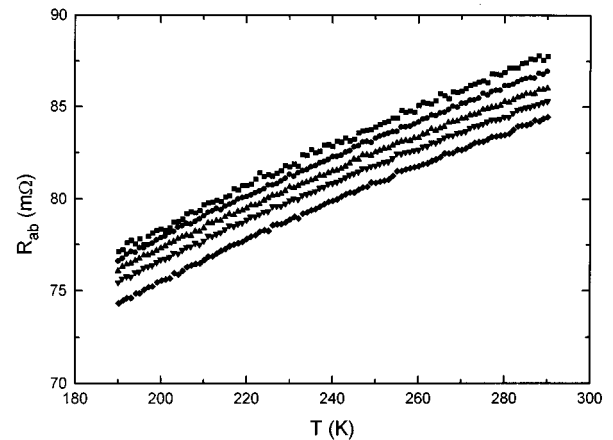


FIG. 5. Linear part of the in-plane R - T curve of textured $\text{Bi}_2\text{Sr}_2\text{CaCu}_2\text{O}_{8+y}$ under selected pressures. Solid squares, $P=10^{-4}$ GPa; solid circle $P=0.14$ GPa; upper-triangle, $P=0.35$ GPa; down-triangle, $P=0.53$ GPa; solid diamond, $P=0.71$ GPa.

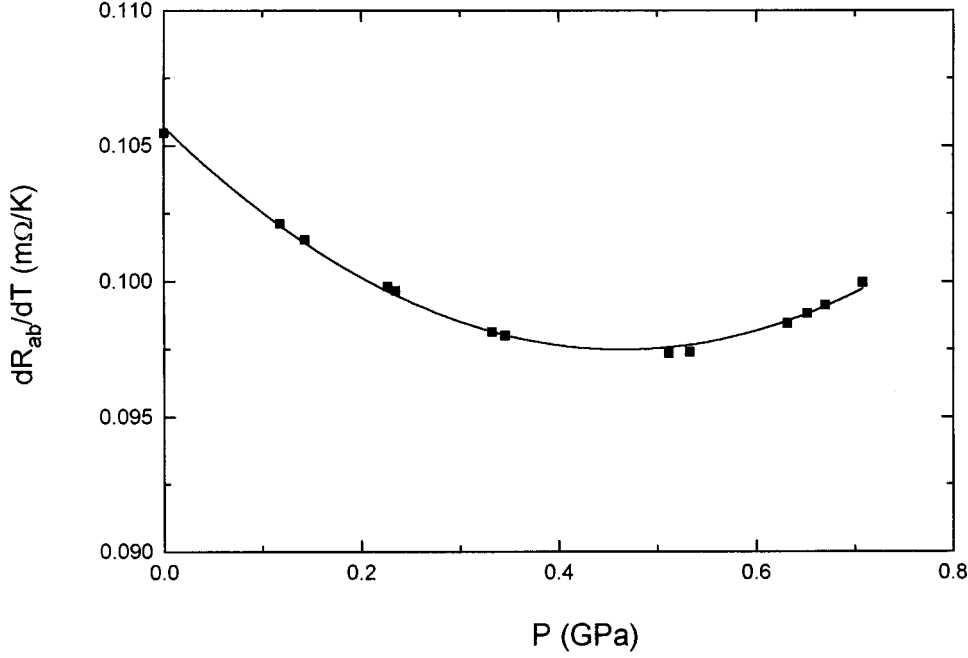


FIG. 6. The pressure dependence of the temperature derivative dR_{ab}/dT of the in-plane normal-state resistance in the linear part of the R - T curve for textured $\text{Bi}_2\text{Sr}_2\text{CaCu}_2\text{O}_{8+y}$. The line shows a parabolic fit.

IV. DISCUSSION AND ANALYSIS

A. The normal-state resistance

The pressure derivative $d \ln \rho_{ab}/dP$ ($= -8.4\% \pm 0.2 \text{ GPa}^{-1}$) obtained here for textured $\text{Bi}_2\text{Sr}_2\text{CaCu}_2\text{O}_{8+y}$ is similar to that (-7.5%) of $\text{Bi}_2\text{Sr}_2\text{CaCu}_2\text{O}_{8+y}$ crystals.¹¹ Both these values are smaller than those of monocrystalline $\text{Bi}_{2.2}(\text{Sr,Ca})_{2.8}\text{Cu}_2\text{O}_{8+y}$ ($-25.5\% \text{ GPa}^{-1}$) and $\text{Bi}_2\text{Sr}_2\text{CaCu}_2\text{O}_{8+y}$ (-15.0%) (Ref. 12) and that ($-11\% \text{ GPa}^{-1}$) of sintered $(\text{BiPb})\text{SrCaCuO}$.¹³ Values of -8.4 and -12.0% have been found for two $\text{Bi}_{2.2}\text{Sr}_{1.8}\text{CaCu}_2\text{O}_{8+y}$ single crystals.⁹

From elementary electron transport theory the volume derivative $d \ln \rho/d \ln V$ of the normal-state resistivity is given by¹

$$\begin{aligned} \frac{d \ln \rho}{d \ln V} &= 2\gamma + B^T \frac{d \ln \delta}{dP} - \frac{d \ln t}{dP} \left(\frac{d \ln V}{dP} \right)^{-1} \\ &= 2\gamma + B^T \frac{d \ln \delta}{dP} - \frac{\beta_c}{\beta_V} \end{aligned} \quad (3)$$

for $T > \Theta$ (the Debye temperature). Here γ is the thermal Grüneisen parameter, δ is the mobile charge carrier density, and β_V is the isothermal volume compressibility, the reciprocal of the bulk modulus B^T . The first term represents the effects from the lattice vibration scattering, the second the effects of the pressure dependence of the mobile charge carrier density, and the third the changes in physical dimensions under pressure. The value of $d \ln \rho_{ab}/d \ln V$, estimated using Eq. (3), is only 64% of that measured for monocrystalline

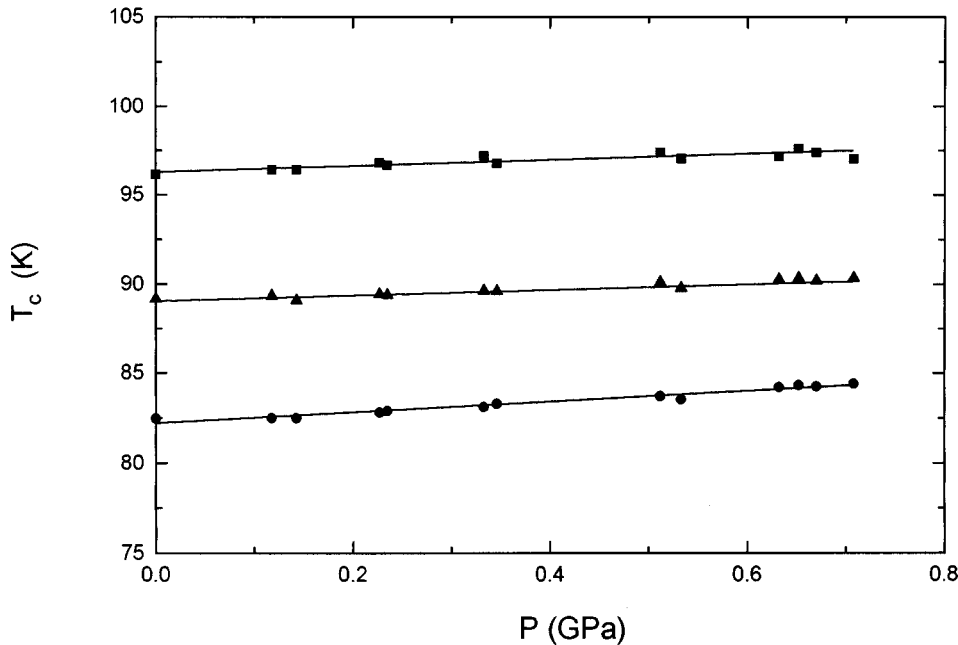


FIG. 7. The pressure dependence of the superconducting transition temperature for textured $\text{Bi}_2\text{Sr}_2\text{CaCu}_2\text{O}_{8+y}$. Solid squares, $T_c(\text{onset})$; solid triangles, $T_c(\text{mid})$; solid circles, $T_c(\text{offset})$; solid lines, linear regression fit.

$\text{Bi}_{2.2}(\text{Sr,Ca})_{2.8}\text{Cu}_2\text{O}_{8+y}$ whereas for some $\text{Bi}_2\text{Sr}_2\text{CaCu}_2\text{O}_{8+y}$ and $\text{YBa}_2\text{Cu}_3\text{O}_{7-x}$ single crystals the calculated values are close to those determined experimentally.¹ The mobile charge carrier term contributes about 75% of the estimated $d \ln \rho_{ab}/d \ln V$ for $\text{Bi}_{2.2}(\text{Sr,Ca})_{2.8}\text{Cu}_2\text{O}_{8+y}$ and $\text{YBa}_2\text{Cu}_3\text{O}_{7-x}$ single crystals.¹ Contributions from the third term are negligible for single crystals. Now $d \ln \rho_{ab}/d \ln V$ can be obtained from the measured pressure derivative $d \ln \rho_{ab}/d \ln P$, using

$$\frac{d \ln \rho_{ab}}{d \ln V} = -B^T \frac{d \ln \rho_{ab}}{d P}. \quad (4)$$

For textured $\text{Bi}_2\text{Sr}_2\text{CaCu}_2\text{O}_{8+y}$ $d \ln R_{ab}/d \ln V$ has been obtained as 2.01 ± 0.06 , using the isothermal bulk modulus $B^T \approx B^S = 31.9$ GPa determined by Saunders *et al.*¹⁴ for very dense textured $\text{Bi}_2\text{Sr}_2\text{CaCu}_2\text{O}_{8+y}$. In general, the elastic stiffnesses of the high-temperature superconducting cuprate ceramics, especially for the bismuth-based materials are small. The elastic stiffnesses of textured $\text{Bi}_2\text{Sr}_2\text{CaCu}_2\text{O}_{8+y}$ are substantially smaller than those for monocrystalline material. For single-crystal Bi2212, the bulk modulus is about 70 GPa; the reduced stiffness of the textured ceramic is due to the microstructural defects including porosity and granularity.¹⁵ The value obtained for $d \ln R_{ab}/d \ln V$ is much smaller than that (18.6) for monocrystalline $\text{Bi}_{2.2}(\text{Sr,Ca})_{2.8}\text{Cu}_2\text{O}_{8+y}$ and those 5.47 and 10.95 estimated for two $\text{Bi}_2\text{Sr}_2\text{CaCu}_2\text{O}_{8+y}$ single crystals.¹

Taking $\gamma = 1.56$,¹ $d \ln \delta/dP = 10.8\% \text{ GPa}^{-1}$,¹⁶ $B^T = 31.9$ GPa, and $\beta_c = 0.021 \text{ GPa}^{-1}$ for textured $\text{Bi}_2\text{Sr}_2\text{CaCu}_2\text{O}_{8+y}$, the value of $d \ln R_{ab}/d \ln V$ calculated using Eq. (3) is 5.89, much larger than that (2.01 ± 0.06) determined for textured $\text{Bi}_2\text{Sr}_2\text{CaCu}_2\text{O}_{8+y}$. If the bulk modulus B^T of 70 GPa for $\text{Bi}_2\text{Sr}_2\text{CaCu}_2\text{O}_{8+y}$ single crystals is used, Eq. (4) gives 4.41 for $d \ln R_{ab}/d \ln V$ using the experimentally determined $d \ln R_{ab}/d P$, while Eq. (3) gives $d \ln R_{ab}/d \ln V$ as 10.0. Hence the small value of $d \ln R_{ab}/d \ln V$ determined for textured $\text{Bi}_2\text{Sr}_2\text{CaCu}_2\text{O}_{8+y}$ cannot be attributed completely to the small value of its bulk modulus B^T . The anomalously small value of $d \ln R_{ab}/d \ln V$ determined for textured $\text{Bi}_2\text{Sr}_2\text{CaCu}_2\text{O}_{8+y}$ indicates that the volume dependence of the normal-state ab -plane resistance due to the lattice vibrational scattering and the pressure dependence of the mobile charge carrier density are smaller than that for single-crystal material.

The Grüneisen parameter γ in Eq. (3) is defined by $-d \ln \Theta/d \ln V$, which is proportional to the reciprocal of the lattice vibrational mean-square amplitude $\overline{X^2}$. Hence γ is proportional to $d \ln \overline{X^2}/d \ln V$. Part of the reason for the small value found for $d \ln R_{ab}/d \ln V$ may lie in a relatively small change of $\overline{X^2}$ under pressure. Ceramic materials contain pores and microcracks which close under pressure,¹⁷⁻¹⁹ reducing the value of the bulk modulus. The thermal Grüneisen parameter γ can be calculated using

$$\gamma = \frac{\alpha B^S}{C_p \rho_m}, \quad (5)$$

where α is the volume thermal expansion coefficient, C_p is the specific heat at constant pressure, and ρ_m is the mass density. Assuming no significant difference in the ratio α/C_p for textured $\text{Bi}_2\text{Sr}_2\text{CaCu}_2\text{O}_{8+y}$ from that for $\text{Bi}_2\text{Sr}_2\text{CaCu}_2\text{O}_{8+y}$ single crystals, substitution of the values

of B^S (31.86 GPa) and ρ_m (95% of theoretical mass density) for textured $\text{Bi}_2\text{Sr}_2\text{CaCu}_2\text{O}_{8+y}$ (Ref. 6) into Eq. (5), gives

$$\frac{\gamma_{\text{eff}}}{\gamma} = \frac{B_t^S \rho_m^S}{B_s^S \rho_m^t} = 0.48, \quad (6)$$

taking B_s^S as 70 GPa. Here the subscript s represents single crystal and t textured material. Taking γ as 1.56, γ_{eff} is 0.75 for textured $\text{Bi}_2\text{Sr}_2\text{CaCu}_2\text{O}_{8+y}$. If γ_{eff} is used in Eq. (6) together with $B^T = 31.86$ GPa and $d \ln \delta/dP = 10.8\% \text{ GPa}^{-1}$, the calculated $d \ln R_{ab}/d \ln V$ is reduced by 27.5% from 5.89 to 4.27, which is still much larger than that (2.01 ± 0.06) determined from the measured $d \ln R_{ab}/d P$. Hence, it is concluded that this discrepancy is not due to defect structure alone.

The pressure dependence of the in-plane resistance is also affected by temperature, particularly when $T < 200$ K (Fig. 4). Below 0.4 GPa the pressure derivative $d \ln R_{ab}/d P$ shows a small linear increase with decreasing temperature between 290 to 200 K, while above 0.4 GPa, it has a slight linear decrease. Information about the temperature dependence of the Grüneisen parameter γ is sparse. White²⁰ has calculated ‘‘average values’’ of γ for several high- T_c superconductors from the experimental data. For the Bi-2:2:1:2 system there is almost no change in γ from 295 K ($\gamma = 1.2$) to 100 K ($\gamma = 1.3$). The temperature dependence of the Hall coefficient R_H for polycrystalline $\text{Bi}_2\text{Sr}_2\text{CaCu}_2\text{O}_{8+y}$ shows no significant change of $d \ln R_H/d P$ with temperature above 120 K.¹⁶ Hence $d \ln R_{ab}/d P$ would not be expected to change with temperature significantly in the normal state [Eq. (3)]. However, our results show that below 200 K, the value of $d \ln R_{ab}/d P$ changes markedly with temperature and its temperature dependence also varies with pressure. These variations in $d \ln R_{ab}/d P$ below 200 K are considered to be caused by the thermodynamic fluctuations of the superconducting order parameter and the pressure effects on these fluctuations.

B. Thermodynamic fluctuations in textured $\text{Bi}_2\text{Sr}_2\text{CaCu}_2\text{O}_{8+y}$

1. At ambient pressure

The rounded shape of the R - T curve and the deviation from linear, metallic behavior above T_c aroused interest soon after the discovery of the high- T_c superconductors^{7,21-29} and are considered to be caused by thermodynamic fluctuations, intrinsic to superconductors. Due to the short coherence length ξ of the order parameter and the high values of T_c , the effects of thermodynamic fluctuations of the superconducting order parameter are particularly pronounced. From studies of the temperature dependence of the resistance it has been suggested that the thermodynamic fluctuations in the R -Ba-Cu-O ($R = \text{Y}$ or Ho , etc.) materials are three dimensional (3D) (Refs. 22-24) but in the Bi-Sr-Ca-Cu-O system are two dimensional (2D).^{7,25,27} A 2D-to-3D crossover in these two systems has been reported.^{8,30,31} Knowledge of the effects of pressure on the thermodynamic fluctuations is sparse. A pressure study of the excess conductivity of $\text{RBa}_2\text{Cu}_3\text{O}_{7-\delta}$ ($R = \text{Y}$, Yb , Gd , and Er) ceramics up to 1.72 GPa has been made,⁸ but no explicit conclusion was reported about the pressure effects on the thermodynamic fluctuations. Han, Dai, and Ren⁶ measured the electrical resistance

of sintered Bi-Pb-Sr-Ca-Cu-O ($T_c=90$ K) under hydrostatic pressure up to 0.7 GPa and concluded that pressure does not seem to change the slope of the R - T curve above T_c . However, the present results for $\text{Bi}_2\text{Sr}_2\text{CaCu}_2\text{O}_{8+y}$ (Fig. 1) provide a basis for estimation of the pressure effects on the thermodynamic fluctuations.

The excess conductivity $\Delta\sigma$ that causes the reduced resistance and the rounding of the transition includes two contributions: $\Delta\sigma=\Delta\sigma_{\text{AL}}+\Delta\sigma_{\text{MT}}$ where (i) $\Delta\sigma_{\text{AL}}$ is the direct Aslamazov-Larkin (AL) contribution,³² attributed to the superconducting pairs created by fluctuations above T_c ,³³ and (ii) $\Delta\sigma_{\text{MT}}$ is the anomalous, Maki-Thompson (MT) contribution,^{34–36} arising from the pair-breaking interactions. According to the time-dependent Ginzburg-Landau (TDGL) theory,³³ the excess conductivity above T_c from the AL contribution should follow a power law:

$$\Delta\sigma_{\text{AL}}(\varepsilon)=C\varepsilon^{-x}, \quad (7)$$

with

$$C=\frac{e^2}{16hd}, \quad x=1 \quad \text{for 2D}, \quad (8)$$

$$C=\frac{e^2}{32h\xi_{\perp,0}}, \quad x=\frac{1}{2} \quad \text{for 3D}. \quad (9)$$

Here $\varepsilon\equiv(T-T_c)/T_c$ is the reduced temperature, x is the critical exponent related to the dimension of the fluctuations. C is temperature independent and is inversely proportional to the coherence length $\xi_{\perp,0}$ for 3D fluctuations and to the characteristic thickness d for a 2D system. By using the formalism of Schmidt³⁷ based on the TDGL theory, Lawrence and Doniach³⁸ derived an expression

$$\Delta\sigma_{\text{LD}}=\frac{e^2}{16hd}\varepsilon^{-1}\left[1+\left(\frac{2\xi_{\perp,0}}{d}\right)^2\right]^{-1/2} \quad (10)$$

for the fluctuation-induced in-plane conductivity. For a small interlayer coupling parameter $\alpha=(2\xi_{\perp,0}/d)^2$ the fluctuations are 2D, while for a large one they are 3D. As temperature decreases and approaches T_c the LD approach predicts crossover of the dimensionality of the fluctuations at a temperature T_0 ,

$$T_0=T_c[1+(2\xi_{\perp,0}/d)^2]. \quad (11)$$

The indirect (MT) contribution for the 2D fluctuations can be expressed as³²

$$\Delta\sigma_{\text{MT}}^{\text{2D}}=\frac{e^2}{8hd}\frac{1}{\varepsilon-\delta}\ln\left(\frac{\varepsilon}{\delta}\right), \quad (12)$$

where $\delta\equiv(T_{co}-T_c)/T_c$ is the pair-breaking parameter and T_{co} corresponds to the critical temperature in the absence of pair-breaking mechanisms.

A common approach to the analysis of the AL contribution [Eqs. (7)–(9)] is to extract the slope of a logarithmic plot of the excess conductivity with respect to ε . The results are sensitive to the value of T_c and can differ substantially²⁹ because of the uncertainty in the values of T_c determined by different methods. To avoid this problem, the fitting procedure

used here has been performed with respect to temperature T , with 290 K as a reference point, rather than ε . From Eq. (7) it can be shown that

$$\left(\frac{\sigma_{290}}{\Delta\sigma_{\text{AL}}}\right)^{1/x}=\left(\frac{\sigma_{290}}{C}\right)^{1/x}\varepsilon=-\left(\frac{\sigma_{290}}{C}\right)^{1/x}+\left(\frac{\sigma_{290}}{C}\right)^{1/x}\frac{T}{T_c}. \quad (13)$$

Hence $(\sigma_{290}/\Delta\sigma_{\text{AL}})^{1/x}$ is linear with respect to T . The reduced excess conductivity $\Delta\sigma/\sigma_{290}$ is calculated from the experimental data as $\Delta\sigma/\sigma_{290}=R_{290}/R(T)-R_{290}/R_N(T)$. The background resistance $R_N(T)=a+bT$ is extrapolated by fitting the linear part of the measured resistance $R(T)$ data above 190 K. In Fig. 8(a), $(\sigma_{290}/\Delta\sigma)^2$ ($x=1/2$) and $(\sigma_{290}/\Delta\sigma)$ ($x=1$) are plotted against temperature up to 140 and 190 K, respectively, for textured $\text{Bi}_2\text{Sr}_2\text{CaCu}_2\text{O}_{8+y}$ at atmospheric pressure. Above T_c both $(\sigma_{290}/\Delta\sigma)$ and $(\sigma_{290}/\Delta\sigma)^2$ increase rapidly as temperature increases. An enlarged scale [Fig. 8(b)] (solid line) shows that in the temperature range T_c+5 K to T_c+20 K (i.e., 94.3–110 K) $(\sigma_{290}/\Delta\sigma)$ is linearly dependent upon temperature; below 94.3 K, closer to T_c , there is a departure from linearity: $(\sigma_{290}/\Delta\sigma)$ goes below the straight line. The linear part in the $(\sigma_{290}/\Delta\sigma)$ - T curve suggests that there is a 2D-AL contribution. However the linear region in the $(\sigma_{290}/\Delta\sigma)^2$ - T from about 94–100 K, Fig. 8(b) (dotted line) implies the existence of 3D fluctuations in that temperature range and introduces difficulties in defining the dimensionality of the fluctuations in the temperature region above T_c and below about 100 K. In this situation it is necessary to check the fits; to do this the differences between $(\sigma_{290}/\Delta\sigma_{\text{AL}})^{1/x}$ and the fitted lines are plotted in Fig. 8(c) as a function of temperature for $x=1/2$ and 1, respectively. The difference between $(\sigma_{290}/\Delta\sigma)$ and the fitted line is almost equal to zero from about T_c to 115 K: in the region above T_c and below 115 K the fluctuations are characterized by two dimensions. By contrast the difference between $(\sigma_{290}/\Delta\sigma)^2$ and its fitted line is close to zero only in the small temperature range from about 94 to 100 K in which the 3D model also fits. Thus the thermodynamic fluctuations probably have 2D character in the textured material.

The characteristic thickness d and the mean-field critical temperature T_c^m can be calculated using Eqs. (13) and (18) from the intercept and slope of the linear fit to the $(\sigma_{290}/\Delta\sigma)$ - T curve. At atmospheric pressure $d=4.5\pm 0.2$ Å and $T_c^m=86.0\pm 0.5$ K. It may be noted here that T_c^m is about 3° lower than T_c (mid) but about 3.5° higher than T_c (offset). This value of d is similar to that (≈ 6 Å) determined³⁹ for a $\text{Bi}_2\text{Sr}_2\text{CaCu}_2\text{O}_{8+y}$ single crystal, using the 2D-AL approach. If the fluctuations from 94 to 100 K are assumed to have 3D character, as the linearity of $(\sigma_{290}/\Delta\sigma)^2$ with temperature T might suggest, the zero-coherence length $\xi_{\perp,0}$ estimated using Eqs. (12) and (16) is 1.2 ± 0.1 Å, close to those determined for polycrystalline $\text{Bi}_2\text{Sr}_2\text{CaCu}_2\text{O}_{8+y}$ (1.46 Å),³¹ $\text{Bi}_2\text{Sr}_2\text{Ca}_2\text{Cu}_3\text{O}_{10+y}$ (1.3 Å),⁴⁰ and $\text{Bi}_2\text{Sr}_2\text{CaCu}_2\text{O}_{8+y}$ (1 Å for the extrapolated $\xi_{\perp,0}$).^{41,42}

To ascertain whether there is a dimensional crossover of the fluctuations in textured $\text{Bi}_2\text{Sr}_2\text{CaCu}_2\text{O}_{8+y}$, the LD approach has been used by fitting Eq. (10) to the reduced excess conductivity $(\Delta\sigma/\sigma_{290})$. A crossover temperature of $T_o=96.1\pm 0.4$ K (at atmospheric pressure) is obtained, which is about 7 K higher than T_c (mid) and about 4 K lower than the starting temperature of the linear part of the

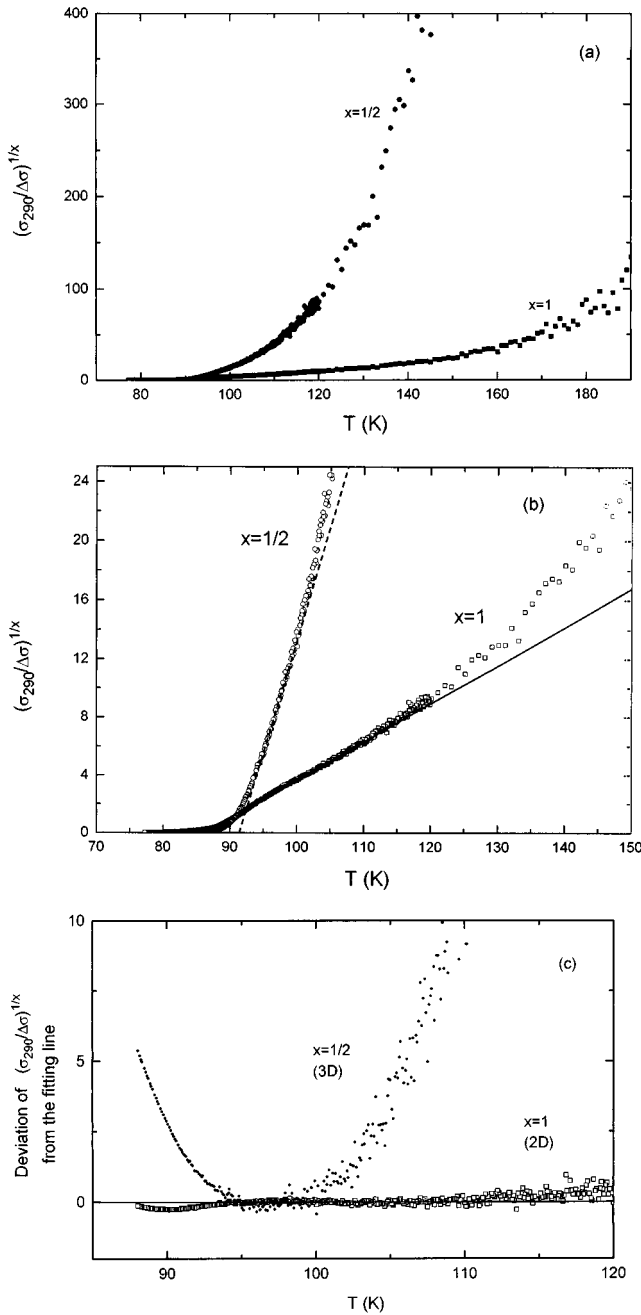


FIG. 8. The temperature dependence of $(\sigma_{290}/\Delta\sigma)^{1/x}$ in the ab plane for textured $\text{Bi}_2\text{Sr}_2\text{CaCu}_2\text{O}_{8+y}$ at atmospheric pressure. (a) For T up to 190 K. Solid squares, the data for $x=1$; solid circles, the data for $x=1/2$. (b) The linear fitting for $(\sigma_{290}/\Delta\sigma)$ - and $(\sigma_{290}/\Delta\sigma)^2 - T$ curves. Open squares, the data for $x=1$; open circles, the data for $x=1/2$. (c) The difference between $(\sigma_{290}/\Delta\sigma)^{1/x}$ and fitted lines for $x=1/2$ (open squares) and $x=1$ (solid circles). The solid line indicates the zero difference.

$(\sigma_{290}/\Delta\sigma)^2 - T$ curve. The characteristic thickness d and the zero-coherence length $\xi_{\perp,0}$, determined by fitting Eq. (10), are, respectively, $4.8 \pm 0.2 \text{ \AA}$, close to that ($4.5 \pm 0.2 \text{ \AA}$) obtained from the linear fit to $(\sigma_{290}/\Delta\sigma)$, and $0.67 \pm 0.03 \text{ \AA}$, smaller than that obtained by using the 3D-AL approach. Recently, Hussy *et al.*⁴³ have estimated $\xi_{\perp,0} < 0.5 \text{ \AA}$ for $\text{Bi}_2\text{Sr}_2\text{CaCu}_2\text{O}_{8+y}$. The behavior of $(\sigma_{290}/\Delta\sigma)$ with temperature, expected from the LD approach, calculated taking the

characteristic thickness d as $4.8 \pm 0.2 \text{ \AA}$ and the zero-coherence length $\xi_{\perp,0}$ as $0.67 \pm 0.03 \text{ \AA}$, is compared with the experimental data in Fig. 9. The line drawn using the LD approach fits the data well from 90 to 110 K. Crossover from 2D to 3D is not clearly defined.

To estimate the indirect (MT) contribution to the thermodynamic fluctuations in textured $\text{Bi}_2\text{Sr}_2\text{CaCu}_2\text{O}_{8+y}$, Eq. (12) and Eq. (2b) quoted by Gauzzi and Pavuna²⁹ have been used to fit the excess conductivity from 90 to 120 K. The characteristic thickness d obtained is about ten times larger ($35\text{--}51 \text{ \AA}$) than those obtained by using the AL and LD approaches. Freitas, Tsuei, and Plaskett²² and Gauzzi and Pavuna²⁹ found no MT contribution in $\text{YBa}_2\text{Cu}_3\text{O}_{7-\delta}$ superconductors in a zero magnetic field. A similar analysis rules out any MT contribution to the thermodynamic fluctuations in textured $\text{Bi}_2\text{Sr}_2\text{CaCu}_2\text{O}_{8+y}$ in a zero magnetic field.

Analysis of their data for $\text{YBa}_2\text{Cu}_3\text{O}_{7-\delta}$ films, led Gauzzi and Pavuna^{29,44} to question the validity of the AL and LD approaches for high- T_c cuprates. They concluded that the critical exponent does not exhibit any universal behavior in the fluctuation region accessible to their experiments. Using a generalized AL expression with a short-wavelength cutoff approach, Gauzzi⁴⁵ derived relations for the in-plane excess conductivity for the 2D and 3D fluctuations. Gauzzi and Pavuna^{29,44} found that the 3D equation fitted the excess conductivity determined for $\text{YBa}_2\text{Cu}_3\text{O}_{7-\delta}$ films well. In contrast to a consensus that the thermodynamic fluctuations in $\text{Bi}_2\text{Sr}_2\text{CaCu}_2\text{O}_{8+y}$ are characterized by two-dimensional behavior, a fit of Gauzzi's equations to the data obtained here for textured $\text{Bi}_2\text{Sr}_2\text{CaCu}_2\text{O}_{8+y}$ indicates failure of the 2D equation. However there is a good fit to the measured data from about 120 to 90 K using Gauzzi's 3D equation (Fig. 9). At atmospheric pressure, Gauzzi's 3D approach leads to $\xi_{\perp,0} \approx 0.43 \pm 0.05 \text{ \AA}$, which is less than those obtained by using the AL ($1.2 \pm 0.1 \text{ \AA}$) and LD ($0.67 \pm 0.03 \text{ \AA}$) approaches, but agrees with the estimate by Hussy *et al.*⁴³

2. Effect of pressure

Application of pressure is found to have a strong influence on the thermodynamic fluctuations in textured $\text{Bi}_2\text{Sr}_2\text{CaCu}_2\text{O}_{8+y}$. The relative change $\delta(\Delta\sigma/\sigma_{290})_P / (\Delta\sigma/\sigma_{290})_{P=0}$ in the reduced excess conductivity is plotted in Fig. 10 as a function of pressure for selected values of $\ln \epsilon$. There is a minimum at about 0.23 GPa. Well above T_c , $\delta(\Delta\sigma/\sigma_{290}) / (\Delta\sigma/\sigma_{290})_{P=0}$ increases almost linearly with increasing pressure when $P > 0.23$ GPa. The changes in $\Delta\sigma/\sigma_{290}$ caused by applying pressure are reduced as T approaches T_c ($\ln \epsilon$ becomes more negative). When $\ln \epsilon > -1$, the reduced excess conductivity $\Delta\sigma/\sigma_{290}$ increases by about 20% at 0.71 GPa. In the context of the AL contribution to the thermodynamic fluctuations, this means that applying pressure enhances the creation of the fluctuation superconducting quasiparticles well above T_c resulting in a larger excess conductivity and the change in the shape of the R - T curve under pressure (Fig. 1). The pressure dependences of the characteristic thickness d , obtained from the 2D-AL and LD approaches, are plotted in Fig. 11(a). Both methods show similar behavior for d : a nonlinear pressure dependence with a maximum at about 0.23 GPa corresponding to the minimum in $\delta(\Delta\sigma/\sigma_{290}) / (\Delta\sigma/\sigma_{290})_{P=0}$ (Fig. 10). Therefore, the pressure derivative of d changes with respect to pressure: 4.7

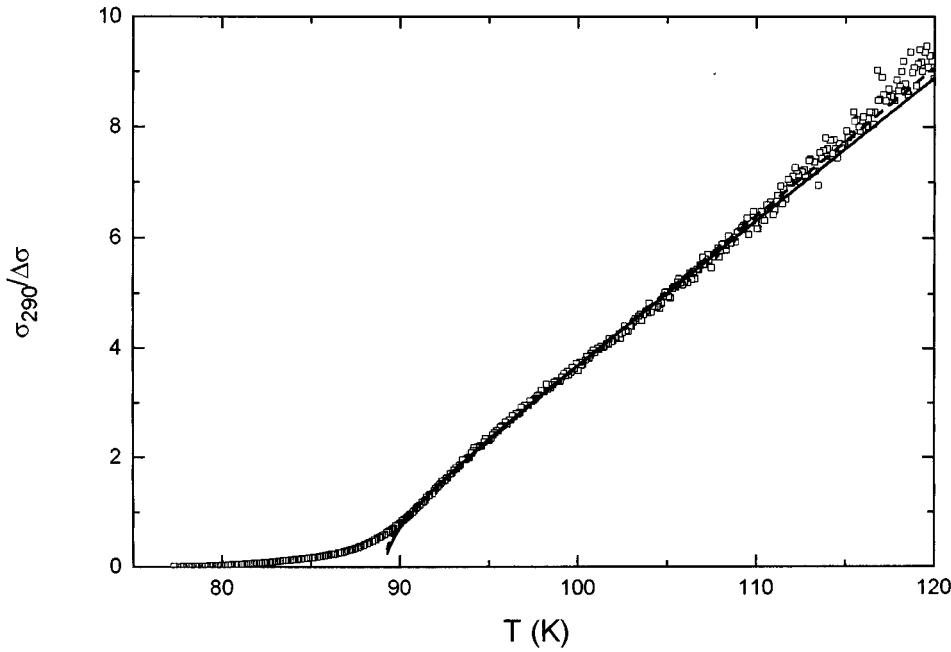


FIG. 9. Fits of the LD (solid line) and Gauzzi's 3D (dashed line) approaches to the experimental $(\sigma_{290}/\Delta\sigma)-T$ (open squares).

± 0.9 and $2.6 \pm 0.8 \text{ \AA GPa}^{-1}$ at 0 GPa from the AL and LD approaches, respectively and at 0.71 GPa -8.4 ± 0.9 and $-3.0 \pm 0.8 \text{ \AA GPa}^{-1}$. Hence, in textured $\text{Bi}_2\text{Sr}_2\text{CaCu}_2\text{O}_{8+y}$ application of pressure appears to have a significant influence on the characteristic thickness d . According to the 2D-AL approach [Eqs. (10) and (11)], the excess conductivity $\Delta\sigma$ is proportional to the reciprocal of d : when d increases with pressure, the reduced excess conductivity $\Delta\sigma/\sigma_{290}$ decreases. Since d decreases with pressure, $\Delta\sigma/\sigma_{290}$ increases. The 2D fluctuations are pressure dependent.

If the 3D fluctuations are assumed to exist between 94 and 100 K, the pressure dependence of the zero-coherence length $\xi_{\perp,0}$ can be obtained by using the 3D-AL, LD, and 3D-Gauzzi approaches, giving the results in Fig. 11(b). Applica-

tion of pressure induces smaller changes on $\xi_{\perp,0}$ than on d . The 3D-AL approach indicates that $\xi_{\perp,0}$ decreases as pressure increases while on the basis of the LD and 3D-Gauzzi approaches it remains almost constant; the pressure derivative $(d\xi_{\perp,0}/dP)_{P=0}$ is $-0.3 \pm 0.1 \text{ \AA GPa}^{-1}$ (AL), $0.01 \pm 0.02 \text{ \AA GPa}^{-1}$ (LD), and $0.09 \pm 0.03 \text{ \AA GPa}^{-1}$; possible 3D fluctuations are almost independent of pressure.

3. Pressure effects on the superconducting transition temperature

The pressure derivative dT_c^{mid}/dP of the superconducting transition temperature T_c^{mid} ($=89.2 \pm 0.2 \text{ K}$ at 10^{-4} GPa) has been determined as $1.8 \pm 0.2 \text{ K GPa}^{-1}$ for textured

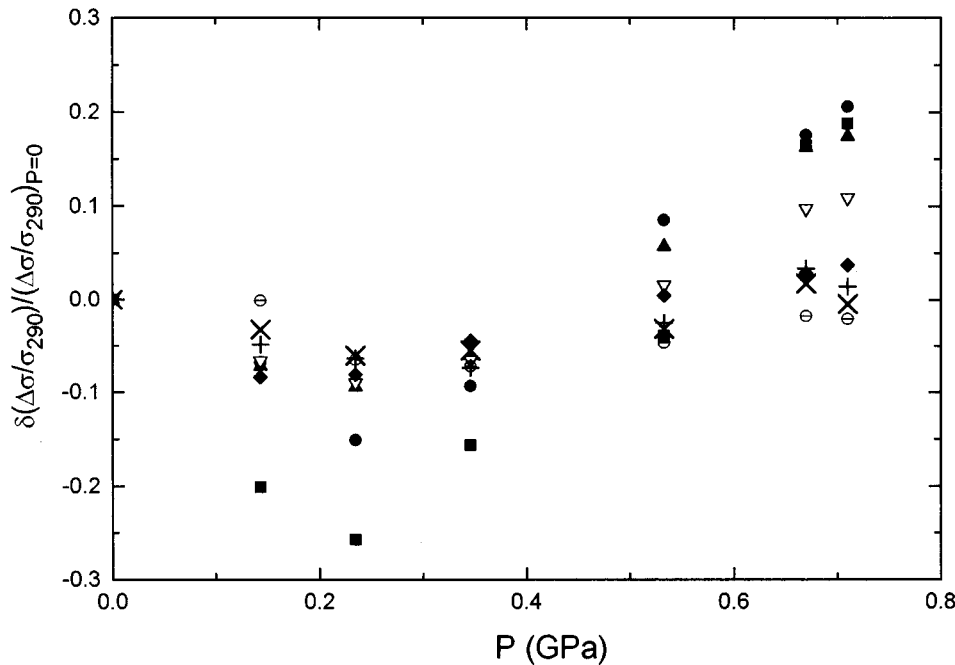


FIG. 10. Pressure dependence of the relative change $\delta(\Delta\sigma/\sigma_{290})/(\Delta\sigma/\sigma_{290})_{P=0}$ in reduced excess conductivity $\Delta\sigma/\sigma_{290}$ at selected reduced-temperatures $\ln \epsilon$ ($\equiv \ln[(T - T_c)/T_c]$). Solid squares, $\ln \epsilon = 0$; solid circles, $\ln \epsilon = -0.5$; solid upper-triangles, $\ln \epsilon = -1$; open down-triangles, $\ln \epsilon = -1.5$; solid diamonds, $\ln \epsilon = -2$; +, $\ln \epsilon = -2.5$; \times , $\ln \epsilon = -3$; barred-open circles, $\ln \epsilon = -4$.

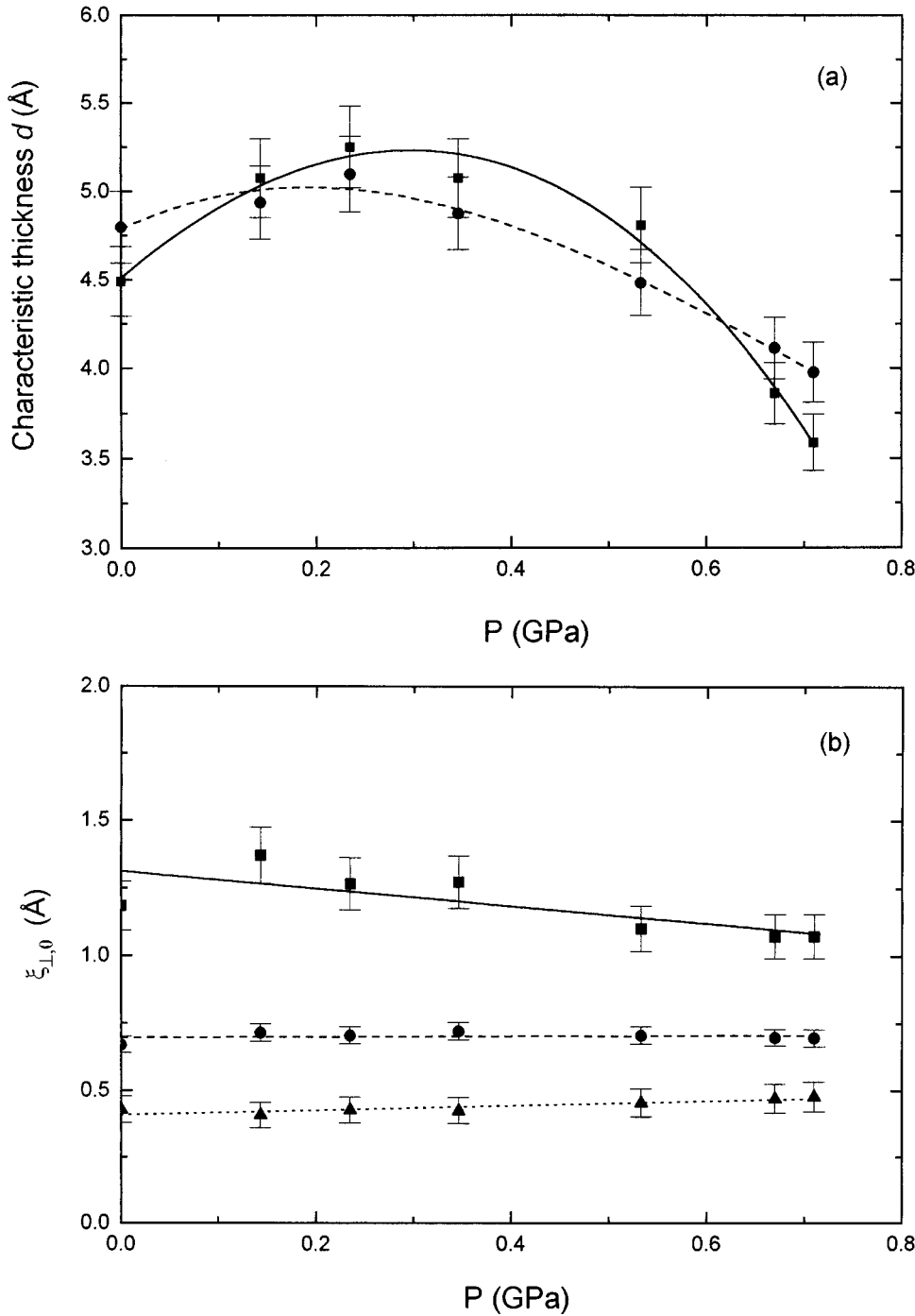


FIG. 11. The pressure dependence of (a) the characteristic thickness d for 2D system obtained from the 2D-AL approach (solid squares) and the LD approach (solid circles), respectively, and (b) the zero-coherence length $\xi_{\perp,0}$ determined by using the 3D-AL approach (solid squares), the LD approach (solid circles), and the 3D-Gauzzi approach (solid triangles), for textured $\text{Bi}_2\text{Sr}_2\text{CaCu}_2\text{O}_{8+y}$. The lines are visual guides.

$\text{Bi}_2\text{Sr}_2\text{CaCu}_2\text{O}_{8+y}$ in the range $(1.3-2.4 \text{ K GPa}^{-1})$ found for most Bi-2:2:1:2 superconductors with an applied pressure of less than 2 GPa (see Table II in Ref. 1) irrespective of the sample morphology (i.e., single crystal, sintered, or textured) and quality. This implies that in polycrystalline materials dT_c/dP is mainly determined by the intra-granular superconducting state. To compare the experimental results with theoretical predictions, it is necessary to transform the pressure derivative dT_c/dP of the superconducting transitions temperature T_c into the volume derivative using

$$\frac{d \ln T_c}{d \ln V} = - \frac{B^T}{T_c} \frac{dT_c}{dP}. \quad (14)$$

To determine $d \ln T_c / d \ln V$, a parameter intrinsic to a superconductor, the value of B^T for a single crystal should be used. Using $B^T = 70$ GPa for $\text{Bi}_2\text{Sr}_2\text{CaCu}_2\text{O}_{8+y}$ single crystals,¹⁴ and the values for $T_c(\text{mid})$ and dT_c^{mid}/dP , gives $d \ln T_c / d \ln V$ for textured $\text{Bi}_2\text{Sr}_2\text{CaCu}_2\text{O}_{8+y}$ as -1.4 : close to that (-1.5) for monocrystalline $\text{Bi}_{2.2}(\text{Sr,Ca})_{2.8}\text{Cu}_2\text{O}_{8+y}$. The pressure-induced increase in T_c has been attributed to the volume dependence of the electron-phonon interaction parameter η in the BCS theory or to the volume dependence of the width of the electron band for a 2D square lattice.^{1,46} The value (-1.4) of $d \ln T_c / d \ln V$ obtained here for $\text{Bi}_2\text{Sr}_2\text{CaCu}_2\text{O}_{8+y}$ falls between those predicted by the BCS (-1) and the RVB (-2) theories,⁴⁶ as found previously for monocrystalline $\text{Bi}_{2.2}(\text{Sr,Ca})_{2.8}\text{Cu}_2\text{O}_{8+y}$.¹

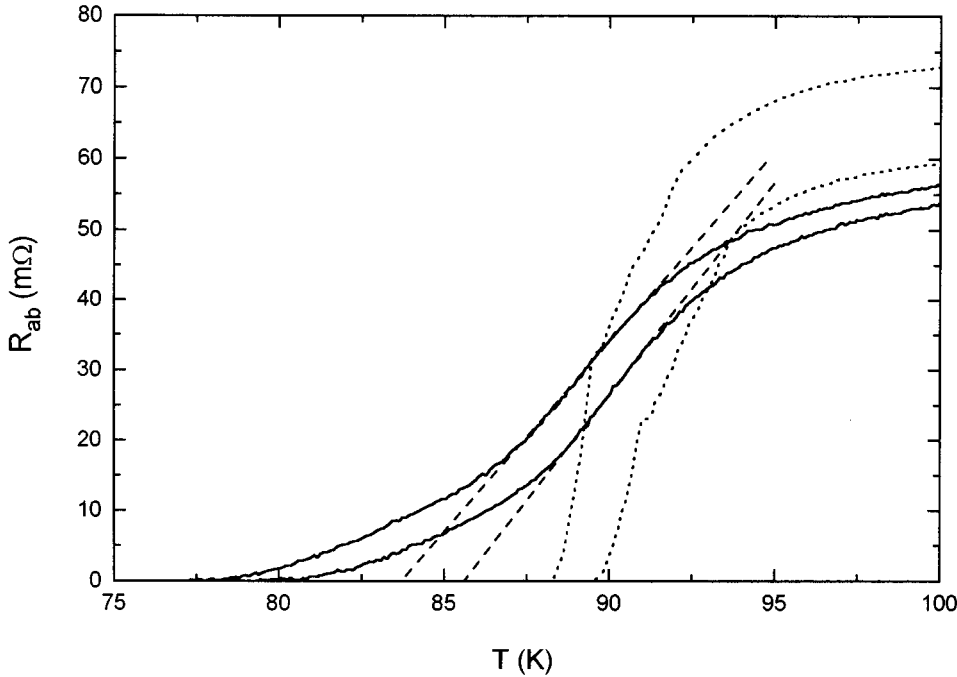


FIG. 12. Comparison of the R - T curves of textured $\text{Bi}_2\text{Sr}_2\text{CaCu}_2\text{O}_{8+y}$ (solid lines) with those of monocrystalline $\text{Bi}_{2.2}(\text{Sr,Ca})_{2.8}\text{Cu}_2\text{O}_{8+y}$ (dotted lines) at 10^{-4} and 0.71 GPa respectively. Dashed lines show the linear regression made for determination of T_d .

C. Pressure effects on the weak links between grain boundaries

Thermodynamic fluctuations are not the sole reason for broadening of the resistive transition in a polycrystalline superconductor; other mechanisms which could cause the broadening include thermally activated flux creep and quantum tunnelling.⁴⁷ The “tail structure” in the R - T or I - V curves in the superconducting transition region is a characteristic of both conventional and high- T_c superconducting materials comprised of grains, such as polycrystalline bulk samples, films and bicrystals.⁴⁷⁻⁵⁰ Tail structures also occur in Josephson junctions made from high- T_c superconductors⁵¹ and have been attributed to weak links at the grain boundaries.²

Information about pressure effects on the weak-link behavior of textured $\text{Bi}_2\text{Sr}_2\text{CaCu}_2\text{O}_{8+y}$ is now obtained. The R - T curves below 100 K for textured $\text{Bi}_2\text{Sr}_2\text{CaCu}_2\text{O}_{8+y}$ and monocrystalline $\text{Bi}_{2.2}(\text{Sr,Ca})_{2.8}\text{Cu}_2\text{O}_{8+y}$ at atmospheric pressure and 0.7 GPa are plotted in Fig. 12. The resistance of both materials drops abruptly at the superconducting transition at almost the same temperature. But there are long tails in the R - T curves for the textured sample. To quantify the spread of the tailing effects, a temperature T_d indicating the departure from the linear behavior in the superconducting transition region is defined. A linear regression, returned with a relative coefficient better than 0.999, is made in the straight line part of the transition region (dashed lines in Fig. 12). At T_d the intragranular resistance reaches zero and the grain-boundary resistance provides the main contribution. At atmospheric pressure T_d is determined as 86.0 ± 0.5 K, higher than $T_c(\text{offset})$ (82.5 K) determined in Sec. II $T_c(\text{offset})$; its pressure derivative is affected by the tail’s pressure dependence.

The resistance tail below T_d has been attributed to the thermal noise in the dc Josephson effect,⁵² i.e., the thermally activated phase slippage in the Josephson effect.^{51,52} The grain boundaries can be likened phenomenologically to ei-

ther a sheath of dirty metal or a layer of insulator.^{51,53} The bonded superconducting grains could form superconductor-insulator-superconductor (S - I - S) junctions or superconductor-(normal metal)-superconductor (S - N - S) junctions. When T approaches T_c from low temperatures, the coupling between the phases of the superconducting order parameter of two superconductors forming a Josephson junction is thermally disrupted and the phase difference between the two superconductors slips.^{51,52} A nonzero time-averaged voltage proportional to the phase-slip rate results; that corresponding to phase slippage of 2π is given by⁵²

$$\bar{V} = \frac{\pi w h}{e}, \quad (15)$$

where w^{-1} is the average time for a phase slippage of 2π . For high- T_c superconductors the thermally activated phase slippage is present over a rather wide temperature range below T_c (Ref. 51) due to the depression of the order parameter at the grain boundaries, which is caused by the short coherence length $\xi(0)$.⁵⁴ Therefore a resistance R_p is produced across the Josephson junction by the phase slippage. The ratio of R_p to the normal-state resistance R_{jn} of the junction is given in the Ambegaokar-Halperin (AH) model⁵² by

$$\frac{R_p}{R_{jn}} = \left[I_0 \left(\frac{\gamma_0}{2} \right) \right]^{-2}. \quad (16)$$

Here I_0 is a modified Bessel function and

$$\gamma_n \propto I_c(T) \quad (17)$$

is the normalized barrier height for the thermally activated phase slip, with $I_c(T)$ being the critical current. Assuming that $I_c(T) \propto (1 - T/T_c)^n$ (Ref. 51) then

$$\gamma_0 = D \left(1 - \frac{T}{T_c} \right)^n. \quad (18)$$

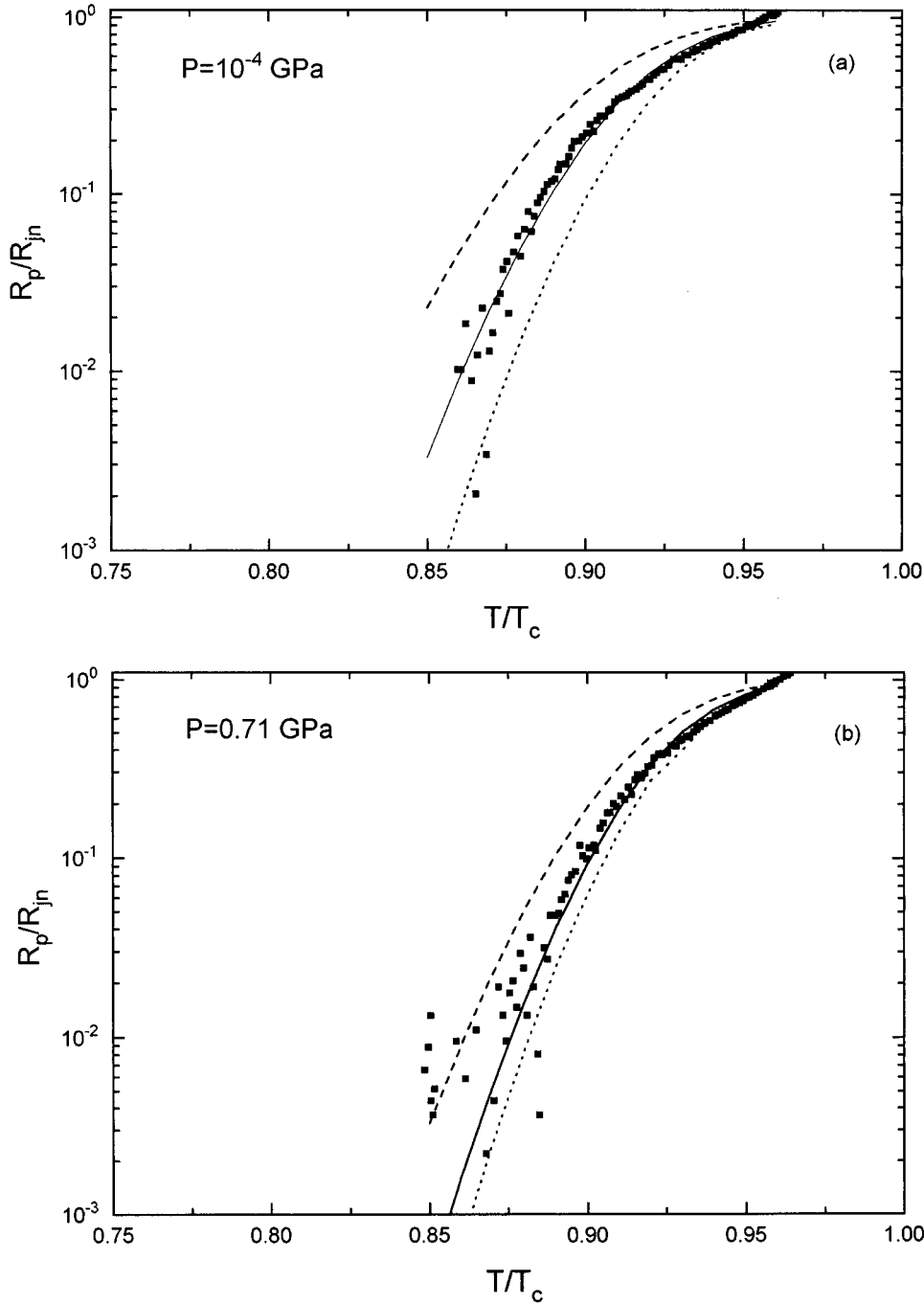


FIG. 13. The reduced temperature (T/T_c) dependence of the normalized resistance R_p/R_{jn} in the tail region for textured $\text{Bi}_2\text{Sr}_2\text{CaCu}_2\text{O}_{8+y}$. Squares, the measured data; lines, AH-model fits with different values for the parameter D . (a) $P=10^{-4}$ GPa. Dashed line, $D=300$; solid line, $D=400$; dotted line, $D=500$. (b) $P=0.71$ GPa. Dashed line, $D=400$; solid line, $D=500$; dotted line, $D=550$.

Fits of Eq. (16) to the normalized resistance R_p/R_{jn} measured under selected pressures, with D and n being the free parameters, are shown in Fig. 13: the fitted lines have been calculated with $n=2$ and T_c determined at each pressure (see Sec. II). The T_c values used to determine the best value of D for the selected pressures are presented in Table I, together with the phase slippage starting temperature T_d . According to the theory for granular superconductors, a value of 2 for the exponent n would correspond to an S - N - S junction.^{55,56} However, the nature of a Josephson junction in high- T_c superconductors is still controversial. According to the Ambegaokar-Baratoff (AB) theory, the critical current density $j_c \propto (1 - T/T_c)$ for a S - I - S junction, while for a S - N - S junction $j_c \propto (1 - T/T_c)^2$.⁵⁶⁻⁵⁸ In studies of the transport properties of high- T_c granular tapes, Okada, Tanaka, and

Kamo⁵⁹ observed that the temperature dependence of the critical current density j_c of a $\text{Bi}_2\text{Sr}_2\text{CaCu}_2\text{O}_{8+y}$ tape with a silver sheath obeyed the granular S - N - S theory. However, analysis of the critical current density in granular Bi(Pb)-Ca-Sr-Cu-O films indicated S - I - S -type behavior for the 2:2:1:2 phase but S - N - S type for the 2:2:3:2 phase; for $\text{YBa}_2\text{Cu}_3\text{O}_{7-\delta}$ films that the junction type could be S - I - S or S - N - S depending on the manufacturing procedure.⁵⁶ Deutscher and Müller⁵⁴ noted that in high- T_c superconductors the short coherence length $\xi(0)$ causes the superconducting order parameter to be depressed at the interface and surface, and that at temperatures close to T_c the decay length of the superconducting wave function in both the insulating and the normal metallic regions is of the order of $\xi(0)$. As a result $j_c \propto (1 - T/T_c)^2$ in both the S - I - S and S - N - S junctions.⁵¹

Considering the energy gap depression in the AB theory, the temperature dependence of the critical current I_c near T_c can be expressed as⁵¹

$$I_c(T) = \frac{\pi \Delta_j^2(0)}{4eR_{jn}k_B T_c} \left(1 - \frac{T}{T_c}\right)^2, \quad (19)$$

where $\Delta_j(0)$ is the energy gap at the interface of the junction at $T=0$ K. By considering Eqs. (17) and (18) and keeping in mind that D is a temperature-independent fitting parameter, we may assume

$$D \propto \frac{\Delta_j^2(0)}{R_{jn}T_c}. \quad (20)$$

Hence a relationship between the pressure derivative of the coefficient D and the energy gap can be derived as

$$\frac{d \ln D}{dP} = 2 \frac{d \ln \Delta_j(0)}{dP} - \frac{d \ln R_{jn}}{dP} - \frac{d \ln T_c}{dP} \quad (21)$$

Therefore, the pressure derivative of the in-plane $\Delta_j(0)$ can be estimated for textured $\text{Bi}_2\text{Sr}_2\text{CaCu}_2\text{O}_{8+y}$. Using the data for R_{jn} (Table I), $d \ln R_{jn}/dP$ has been estimated as $0.087 \pm 0.043 \text{ GPa}^{-1}$ and $d \ln D/dP$ as $0.31 \pm 0.01 \text{ GPa}^{-1}$. Substitution of these values and $0.02 \pm 0.01 \text{ GPa}^{-1}$ for $d \ln T_c^{\text{mid}}/dP$ into Eq. (21) yields $d \ln \Delta_j(0)/dP = 0.12 \pm 0.02 \text{ GPa}^{-1}$, showing how the width of the in-plane energy gap at the interface of the junction increases with increasing pressure. This accounts for the shift of the tail structure in the R - T curve under pressure. With a wider energy gap the barrier height for the thermally activated phase slip is higher. Since a higher thermal energy is required for the phase slip to occur, the resistance R_p produced by the phase slippage at temperatures below T_d decreases with increasing pressure. The resistance tail shifts to higher temperatures accordingly. This is the reason why the pressure derivative dT_c^{off}/dP of textured $\text{Bi}_2\text{Sr}_2\text{CaCu}_2\text{O}_{8+y}$ is larger than that of monocrystalline $\text{Bi}_{2.2}(\text{Sr,Ca})_{2.8}\text{Cu}_2\text{O}_{8+y}$. The decrease in R_p results in an increase in critical current between the grains. Hence grain-boundary linkage is enhanced by pressure. A relationship obtained⁵¹ from the AH model and the AB expression [Eq. (22)],

$$\frac{\Delta T}{T_c} \propto \frac{k_B T_c \sqrt{R_{jn}}}{2 \Delta_j(0)} \quad (22)$$

can be used to check the assumptions used to obtain Eq. (21); ΔT is the superconducting transition width. Using Eq. (22) it can be shown that

$$\frac{d \ln \Delta_j(0)}{dP} = \frac{1}{2} \frac{d \ln R_{jn}}{dP} + 2 \frac{d \ln T_c}{dP} - \frac{d \ln \Delta T}{dP}. \quad (23)$$

In this work $d \ln \Delta T/dP = 0.08 \pm 0.03 \text{ GPa}^{-1}$ is obtained from the pressure dependence of $\Delta T_c(\text{mid})$. From Eq. (23) and the results for $d \ln T_c^{\text{mid}}/dP$ and $d \ln R_{jn}/dP$, we have obtained $d \ln \Delta_j(0)/dP \approx 0.08 \pm 0.05 \text{ GPa}^{-1}$, in reasonable accord with the value ($0.12 \pm 0.05 \text{ GPa}^{-1}$) obtained using Eq. (21).

The values (400–500) of the coefficient D determined for textured $\text{Bi}_2\text{Sr}_2\text{CaCu}_2\text{O}_{8+y}$ are smaller than those determined for $\text{YBa}_2\text{Cu}_3\text{O}_{7-\delta}$ materials. The study of a $\text{YBa}_2\text{Cu}_3\text{O}_{7-\delta}$ grain-boundary Josephson junction provided a value of 1350

for D .⁵¹ From work on transport properties of epitaxial $\text{YBa}_2\text{Cu}_3\text{O}_{7-\delta}$ films, Friedl *et al.*⁶⁰ obtained 800 for D . Wang⁵⁰ quoted a D of 1550 obtained from work on a $\text{YBa}_2\text{Cu}_3\text{O}_{7-\delta}$ bicrystal Josephson junction. Equation (20) indicates that D is proportional to $\Delta_j^2(0)$ and the reciprocal of the product R_{jn} and T_c . In the present work, the value of T_c used is similar to those of the $\text{YBa}_2\text{Cu}_3\text{O}_{7-\delta}$ materials, while that of R_{jn} ($\approx 15 \text{ m}\Omega$ at atmospheric pressure) is much smaller than those ($1\text{--}7.5\Omega$) of the $\text{YBa}_2\text{Cu}_3\text{O}_{7-\delta}$ materials.⁵⁰ This implies that the value of $\Delta_j(0)$ for $\text{Bi}_2\text{Sr}_2\text{CaCu}_2\text{O}_{8+y}$ is 10 times smaller than that of $\text{YBa}_2\text{Cu}_3\text{O}_{7-\delta}$.

V. CONCLUSIONS

Measurements of the pressure dependence of the in-plane normal-state resistance of a textured $\text{Bi}_2\text{Sr}_2\text{CaCu}_2\text{O}_{8+y}$ high- T_c superconductor have been made and compared with those previously reported for monocrystalline $\text{Bi}_{2.2}(\text{Sr,Ca})_{2.8}\text{Cu}_2\text{O}_{8+y}$.¹ While a number of properties are common to both types of material, others are characteristics of the granularity of polycrystalline superconductors.

(1) The pressure derivative $d \ln \rho_{ab}/dP$ of the normal-state in-plane resistivity of textured $\text{Bi}_2\text{Sr}_2\text{CaCu}_2\text{O}_{8+y}$ is $-8.4\% \pm 0.2 \text{ GPa}^{-1}$, similar to that reported for some $\text{Bi}_2\text{Sr}_2\text{CaCu}_2\text{O}_{8+y}$ single crystals but much smaller than that ($-25.5\% \pm 0.2 \text{ GPa}^{-1}$) of monocrystalline $\text{Bi}_{2.2}(\text{Sr,Ca})_{2.8}\text{Cu}_2\text{O}_{8+y}$.¹ The volume derivative $d \ln R_{ab}/d \ln V$ of the normal-state resistance of textured $\text{Bi}_2\text{Sr}_2\text{CaCu}_2\text{O}_{8+y}$ (2.01 ± 0.06) is much smaller than that for $\text{Bi}_2\text{Sr}_2\text{CaCu}_2\text{O}_{8+y}$ single crystals. Part of the reason for this small value is that the pores or cracks in this ceramic material reduce the influence of pressure on the mean-square lattice vibrational amplitude $\overline{X^2}$, and therefore reduce the effective Grüneisen parameter γ_{eff} .

(2) A temperature dependence of $d \ln R_{ab}/dP$ found for textured $\text{Bi}_2\text{Sr}_2\text{CaCu}_2\text{O}_{8+y}$ alone, especially below 200 K, is caused by thermodynamic fluctuations of the superconducting order parameter and is affected by pressure (Fig. 4).

(3) The temperature derivative $d \ln R_{ab}/dT$ extracted from the linear part of the R - T curve between 190 and 290 K is pressure dependent and has a minimum at 0.4 GPa.

(4) The pressure derivatives dT_c/dP of the superconducting transition temperature T_c are determined as 1.6 ± 0.3 , 1.8 ± 0.2 , and $3.0 \pm 0.2 \text{ K GPa}^{-1}$ at the onset, midpoint, and offset of the R - T curve in the transition region, respectively. For textured $\text{Bi}_2\text{Sr}_2\text{CaCu}_2\text{O}_{8+y}$, thermodynamic fluctuations influence the pressure dependence of $T_c(\text{onset})$. The pressure dependence of $T_c(\text{offset})$ is affected by weak links across grain boundaries whilst the pressure derivative of $T_c(\text{mid})$ is unaffected by these effects. The pressure derivative dT_c^{mid}/dP falls in the range measured for most Bi-2:2:1:2 superconductors: in polycrystalline materials dT_c/dP is mainly determined by the intragranular superconducting state, and its value is unaffected by the interactions between grain boundaries under pressure.

(5) A value of -1.4 has been obtained for the volume derivative $d \ln T_c/d \ln V$ of textured $\text{Bi}_2\text{Sr}_2\text{CaCu}_2\text{O}_{8+y}$. This result confirms the previous finding¹ that the value of $d \ln T_c/d \ln V$ for $\text{Bi}_2\text{Sr}_2\text{CaCu}_2\text{O}_{8+y}$ is between the values predicted by the BCS (-1) and the RVB (-2) theories.

TABLE I. The values of the parameters used to determine the coefficient D in Eq. (15) at selected pressures. T_d is the temperature at which the weak-link effects commence. R_{jn} is the normal-state resistance of the junctions across grain boundaries.

P (GPa)	T_c (mid) (± 0.2 K)	D (± 10)	T_d (± 0.5 K)	R_{jn} (± 0.05 m Ω)
10^{-4}	89.2	400	86.0	14.73
0.35	89.6	450	86.6	14.58
0.53	89.8	470	86.9	14.50
0.71	90.4	500	87.5	13.71

(6) The effects of hydrostatic pressure on thermodynamic fluctuations of the superconducting parameter of textured $\text{Bi}_2\text{Sr}_2\text{CaCu}_2\text{O}_{8+y}$ have been investigated. An analysis based on the AL approach shows that the fluctuations have two-dimensional character between T_c and 115 K. However, there is an ambiguity in the dimensionality from 94 to 100 K, which may be caused by the inhomogeneities or disorder of the textured material. Applying hydrostatic pressure enhances the thermodynamic fluctuations. At temperatures when $\ln \epsilon > -1$ the reduced excess conductivity $\Delta\sigma(\epsilon)/\sigma_{290}$ increases by about 20% at 0.71 GPa. As pressure is increased the characteristic thickness d of the 2D system changes nonlinearly. The value of d is reduced by about 20% at a pressure of 0.71 GPa.

(7) Study of the effects of weak links across the grain

boundaries on the resistance in textured $\text{Bi}_2\text{Sr}_2\text{CaCu}_2\text{O}_{8+y}$ shows that the Ambegaokar-Halperin (AH) model fits the reduced temperature dependence of the normalized resistance R_p/R_{jn} in the tail region of the R - T curve. The junctions formed by the superconducting grains and grain boundaries are S - N - S -like with $I_c(T) \propto (1-T/T_c)^2$. Under hydrostatic pressure the temperature T_d , at which a tail structure in the R - T curve starts, increases and the tail structure shifts to higher temperatures. By using the AH model and the Ambegaokar-Baratoff (AB) expression for the critical current,⁵¹ the pressure derivative $d \ln \Delta_j(0)/dP$ of the energy gap $\Delta_j(0)$ at grain boundaries has been estimated as $0.12 \pm 0.02 \text{ GPa}^{-1}$, i.e., the energy gap increases under pressure. Hence under pressure the potential barrier for the thermally activated phase slip of the superconducting parameter between grains gets higher and the resistance R_p produced by the phase slippage at temperatures below T_d decreases with increasing pressure, which results in the shift of the tail structure. The intergrain critical current increases under pressure. The value of $\Delta_j(0)$ for textured $\text{Bi}_2\text{Sr}_2\text{CaCu}_2\text{O}_{8+y}$ is about 10 times smaller than that of $\text{YBa}_2\text{Cu}_3\text{O}_{7-\delta}$.

ACKNOWLEDGMENTS

We are grateful to the Engineering and Physical Research Council (EPSRC) for financial support. We would like to thank K. C. Goretta of the Argonne National Laboratory for supplying the sample of textured $\text{Bi}_2\text{Sr}_2\text{CaCu}_2\text{O}_{8+y}$ and B. Chapman for x-ray-diffraction spectroscopy work.

- ¹H. J. Liu, Q. Wang, G. A. Saunders, D. P. Almond, B. Chapman, and K. Kitahama, *Phys. Rev. B* **51**, 9167 (1995).
- ²R. L. Peterson and J. W. Ekin, *Phys. Rev. B* **37**, 9848 (1988).
- ³C.-Y. Chu, J. L. Routbort, Chen Nan, A. C. Biondo, D. S. Kupperman, and K. C. Goretta, *Supercond. Sci. Technol.* **5**, 306 (1992).
- ⁴F. Chang, P. J. Ford, G. A. Saunders, L. Jiaqiang, D. P. Almond, B. Chapman, M. Cankurtaran, R. B. Poepfel, and K. C. Goretta, *Supercond. Sci. Technol.* **6**, 484 (1993).
- ⁵V. Ilakovac, L. Forro, C. Ayache, and J. Y. Henry, *Phys. Lett.* **161**, 314 (1991).
- ⁶S. H. Han, X. Dai, and R. J. Ren, *Appl. Supercon.* **1**, 451 (1993).
- ⁷M. Akinaga, and L. Rinderer, *Physica B* **165&166**, 1373 (1990).
- ⁸H. A. Borges and M. A. Continentino, *Solid State Commun.* **80**, 197 (1991).
- ⁹Y. Tajima, M. J. Hikita, M. Suzuki, and Y. Hidaka, *Physica C* **158**, 237 (1989).
- ¹⁰S. Klotz and J. S. Schilling, *Physica C* **209**, 499 (1993).
- ¹¹L. Forró, V. Ilakovac and B. Keszei, *Phys. Rev. B* **41**, 9551 (1990).
- ¹²J. Beille, H. Dupendant, O. Laborde, Y. Lefur, M. Perroux, R. Tournier, Y. F. Yen, J. H. Wang, D. N. Zheng, and Z. Zhao, *Physica C* **156**, 448 (1988).
- ¹³J. Kamarád, Z. Arnold, L. Smrcka, T. Suski, and P. Wisniewski, *Supercond. Sci. Technol.* **2**, 269 (1989).
- ¹⁴G. A. Saunders, Chang Fanggao, Li Jiaqiang, Q. Wang, M. Cankurtaran, E. F. Lambson, P. J. Ford, and D. P. Almond, *Phys. Rev. B* **49**, 9862 (1994).
- ¹⁵M. Cankurtaran, G. A. Saunders, J. R. Willis, A. Al-Kheffaji, and D. P. Almond, *Phys. Rev. B* **39**, 2872 (1989).
- ¹⁶C. Murayama, Y. Iye, T. Enomoto, A. Fukushima, N. Móri, Y. Yamada, and T. Matsumoto, *Physica C* **185-189**, 1293 (1991).
- ¹⁷D. J. Holcomb and M. J. Mayo, *J. Mater. Res.* **5**, 1827 (1990).
- ¹⁸S. Rigden, G. K. White, and E. R. Vance, *Phys. Rev. B* **47**, 1153 (1993).
- ¹⁹Q. Wang, G. A. Saunders, D. P. Almond, M. Cankurtaran, and K. C. Goretta, *Phys. Rev. B* **52**, 3711 (1995).
- ²⁰G. K. White, in *Studies of High Temperature Superconductors: Advances in Research and Applications*, edited by A. Narlikar (Nova Science, New York, 1992), Vol. 9, p. 121.
- ²¹J. G. Bednorz and K. A. Müller, *Z. Phys. B* **64**, 189 (1986).
- ²²P. P. Freitas, C. C. Tsuei, and T. S. Plaskett, *Phys. Rev. B* **36**, 833 (1987).
- ²³F. Vidal, J. A. Veira, J. Maza, F. Miguélez, E. Morán, and M. A. Alario, *Solid State Commun.* **66**, 421 (1988).
- ²⁴F. Vidal, J. A. Veira, J. Maza, J. J. Ponte, J. Amador, C. Cascales, M. T. Casais, and I. Rasines, *Physica C* **156**, 165 (1988).
- ²⁵F. Vidal, J. A. Veira, J. Maza, J. J. Ponte, F. García-Alvarado, E. Morán, J. Amador, C. Cascales, A. Castro, M. T. Casais, and I. Rasines, *Physica C* **156**, 807 (1988).
- ²⁶W. Schnelle, E. Braun, H. Broicher, H. Weiss, H. Geus, S. Ruppel, M. Galfy, W. Braunisch, A. Waldorf, F. Seidler, and D. Wohlleben, *Physica C* **161**, 123 (1989).
- ²⁷J. J. Wnuk, L. W. M. Schreurs, P. J. T. Eggenkamp, and P. J. E. M. van der Linden, *Physica B* **165&166**, 1371 (1990).
- ²⁸S. V. Sharma, G. Sinha, T. K. Nath, S. Chakraborty, and A. K.

- Majumdar, *Physica C* **242**, 351 (1995).
- ²⁹A. Gauzzi and D. Pavuna, *Phys. Rev. B* **51**, 15 420 (1995).
- ³⁰P. Mendal, A. Poddar, A. N. Das, B. Ghosh, and P. Choudhury, *Physica C* **169**, 43 (1990).
- ³¹S. Ravi and V. S. Bai, *Solid State Commun.* **83**, 117 (1992).
- ³²L. G. Aslamazov and A. I. Larkin, *Phys. Lett.* **26A**, 238 (1968).
- ³³W. J. Skocpol and M. Tinkham, *Rep. Prog. Phys.* **38**, 1049 (1975).
- ³⁴K. Maki, *Prog. Theor. Phys.* **39**, 897 (1968).
- ³⁵K. Maki, *Prog. Theor. Phys.* **40**, 193 (1968).
- ³⁶R. S. Thompson, *Phys. Rev. B* **1**, 327 (1970).
- ³⁷H. Schimidt, *Z. Phys.* **216**, 336 (1968).
- ³⁸W. E. Lawrence and S. Doniach, in *Proceedings of the 12th International Conference on Low Temperature Physics*, Kyoto, Japan, edited by E. Kanda (Keigaku, Tokyo, 1971), p. 361.
- ³⁹S. Martin, A. T. Fiory, R. M. Fleming, G. P. Espinosa, and A. S. Cooper, *Phys. Rev. Lett.* **62**, 677 (1989).
- ⁴⁰P. De Villiers, R. A. Doyle, and V. V. Gridin, *J. Phys.: Condens. Matter* **4**, 9401 (1992).
- ⁴¹T. T. N. Palstra, B. Batlogg, L. F. Schneemeyer, R. B. van Dover, and J. W. Waszczak, *Phys. Rev. B* **38**, 5102 (1988).
- ⁴²M. J. Naughton, R. C. Yu, P. K. Davies, J. E. Fischer, R. V. Chamberlin, Z. Z. Wang, T. W. Jing, N. P. Ong, and P. M. Chaikin, *Phys. Rev. B* **38**, 9208 (1988).
- ⁴³N. E. Hussey, J. R. Cooper, R. A. Doyle, C. T. Lin, W. Y. Liang and D. C. Sinclair, G. Balakrishnan, D. McK. Paul, and A. Rev-colevschi, *Phys. Rev. B* **53**, 6752 (1996).
- ⁴⁴A. Gauzzi and D. Pavuna, *J. Alloys Comp.* **195**, 647 (1993).
- ⁴⁵A. Gauzzi, *Europhys. Lett.* **21**, 207 (1993).
- ⁴⁶R. Griessen, *Phys. Rev. B* **36**, 5284 (1987).
- ⁴⁷M. Prester, E. Babic, M. Stubicar, and P. Nozar, *Phys. Rev. B* **49**, 6967 (1994).
- ⁴⁸Y. Enomoto, M. Suzuki, T. Murakami, T. Inukai, and T. Inamura, *Jpn. J. Appl. Phys.* **20**, L661 (1981).
- ⁴⁹M. A. Dubson, S. T. Herbert, J. J. Calabrese, D. C. Harris, B. R. Partton, and J. C. Garland, *Phys. Rev. Lett.* **60**, 1061 (1988).
- ⁵⁰S. Wang, in *Studies of High Temperature Superconductors: High T_c SQUIDS and Related Studies*, edited by A. Narlikar (Nova Science, New York, 1994), Vol. 12, p. 121.
- ⁵¹R. Gross, P. Chaudhari, D. Dimos, A. Gupta, and G. Koren, *Phys. Rev. Lett.* **64**, 228 (1990).
- ⁵²V. Ambegaokar and B. I. Halperin, *Phys. Rev. Lett.* **25**, 1364 (1969).
- ⁵³P. Chaudhari, *Physica C* **185-189**, 292 (1991).
- ⁵⁴G. Deutscher and K. A. Müller, *Phys. Rev. Lett.* **59**, 1745 (1987).
- ⁵⁵J. R. Clem B. Bumble, S. I. Raider, W. J. Gallagher, and Y. C. Shih, *Phys. Rev. B* **35**, 6637 (1987).
- ⁵⁶J. W. C. De Vries, G. M. Stollman, and M. A. M. Gijs, *Physica C* **157**, 406 (1989).
- ⁵⁷V. Ambegaokar and A. Baratoff, *Phys. Rev. Lett.* **10**, 486 (1963).
- ⁵⁸V. Ambegaokar and A. Baratoff, *Phys. Rev. Lett.* **11**, 104 (1963).
- ⁵⁹M. Okada, K. Tanaka, and T. Kamo, *Jpn. J. Appl. Phys.* **32**, 2634 (1993).
- ⁶⁰G. Friedl, B. Roas, M. Romheld, L. Schultz, and W. Jutzi, *Appl. Phys. Lett.* **59**, 2751 (1991).